Chem Soc Rev

Cite this: *Chem. Soc. Rev.*, 2012, **41**, 7403–7430

www.rsc.org/csr

CRITICAL REVIEW

Engineering polyoxometalates with emergent properties†

Haralampos N. Miras, Jun Yan, De-Liang Long and Leroy Cronin*

Received 29th May 2012
DOI: 10.1039/c2cs35190k

Polyoxometalates are clusters of metal-oxide units, comprising a large diversity of nanoscale structures, and have many common building blocks; in fact polyoxometalate clusters are perhaps the largest non-biologically derived molecules structurally characterised. Not only can polyoxometalates have gigantic nanoscale molecular structures, but they also a have a vast array of physical properties, many of which can be specifically 'engineered-in'. Here we describe how building block libraries of polyoxometalates can be used to construct systems with important catalytic, electronic, and structural properties. We also show that it is possible to construct complex chemical systems based upon polyoxometalates, manipulating the templating/self templating rules to exhibit emergent processes from the molecular to the macroscopic scale.

1. Introduction

Polyoxometalates (POMs) are anionic metal oxide clusters of Mo, W, V and Nb which have attracted great attention during the last two decades, due to their remarkable structural and electronic/magnetic properties,[1,2] but also to their intriguing applications ranging from catalysis[3] and medicine.[4] The recent surge in the structural development of POM chemistry started in the early 1990s when a comprehensive review article published by Pope and Müller[5] in 1991 noted the interesting features and the potential of this unique class of compounds. The development of polyoxometalate cluster science during the subsequent years was rapid, partly inspired by this 1991 review, and further expanded in 1998 in a special thematic issue of Chemical Reviews.[6] This issue brought together the

WestCHEM, School of Chemistry, University of Glasgow, Glasgow, G12 8QQ, UK. E-mail: Lee.Cronin@glasgow.ac.uk; Web: http://www.croninlab.com

† Part of a themed issue covering the latest developments in polyoxometalate science.

Haralampos N. Miras

Haralampos N. Miras was born in Athens, Greece. He gained his BSc degree in chemistry from Ioannina University and obtained his PhD under the supervision of Prof. T. A. Kabanos at Ioannina University in 2004. In 2005 he moved to the University of Rio Piedras, Puerto Rico, USA to take up a post-doctoral fellowship with Prof. R. G. Raptis in pyrazolate based coordination materials. In 2006 he was offered a research associate position by Prof. Cronin at the University of Glasgow in the area of discovery, synthesis and mechanistic studies using ESI/CSI-MS of large polyoxometalate and coordination clusters. In 2010 was awarded a Royal Society of Edinburgh (RSE) research fellow co-funded by Marie Curie actions. He is currently leader of the complex chemical systems sub-group, within the Cronin group. His research interests are focusing in polyoxometalate, chalcogenide and coordination chemistry.

Jun Yan

Jun Yan was born in China and gained his BSc and MSc degrees in Chemistry at Beijing Institute of Technology. In 2007, he was awarded the overseas scholarship from China Scholarship Council to carry out postgraduate study at the University of Glasgow in the Cronin group. He obtained his PhD degree in 2010 and is currently a post-doctoral research assistant in the Cronin Group. His research interest's span in the range of polyoxometalates, coordination chemistry, electrochemistry, cluster based devices and electronics.

many disparate areas of POM chemistry, including their history, significant developments and several applications. Recently, we updated the literature with reviews in 2007 and 2010 exploring the potential of building functional materials[7] and nanoscale systems.[8] Today we hope that this themed issue of *Chem. Soc. Rev.*, dedicated to the frontiers of metal-oxide polyoxometalate science in which this review is published will act as a catalyst to stimulate the field, helping current POM researchers to work together effectively, and inspiring others to work in this area bringing in new ideas, perspectives, expertise, and young researchers.

Despite the fact that the core-number of POM-based research groups is quite small compared to some areas, the field continues to grow vibrantly in terms of new compounds, interesting structures, and the exploration of POM physical properties. It is crucial that to continue the development of the area, the link between structure and function continues to be probed, developed, and applied. Moreover, novel synthetic approaches (hydrothermal and microwave processing, mixed-solvents, ionic liquids *etc.*) have contributed to the observed rapid expansion of knowledge in POM chemistry.[9] However, frustratingly, the design approaches employed can sometimes only be based on empirical observations, and the fact that speciation as well as the aggregation of metalates, is based on complex condensation processes driven by the concentration of protons in the reaction medium.

2. Building blocks

Generally, the approaches used to produce POM based clusters are simple requiring a small number of steps, or even just one step (one-pot syntheses), during which acidification of an aqueous solution containing the relevant metallic salt of molybdates, tungstates or vanadates drives the condensation process and induces the aggregation of metallic species towards the formation of specific archetypes. The aggregation process though is controlled by a long list of experimental variables, which should be considered when planning the synthesis of a given polyoxometalate archetype, such as: (1) concentration/type of metal oxide anion, (2) pH, (3) ionic strength, (4) heteroatom type/concentration, (5) presence of additional ligands, (6) reducing environment, (7) temperature and pressure of reaction (*e.g.* microwave, hydrothermal, refluxing), (8) counter-ion and metal-ion effect and (9) processing methodology (one-pot, continuous flow conditions,[7] 3d printing of reactionware).[7–10]

Based on the experience developed over the last decades, the vast growth in the number of assembled POM clusters (many of which with an unmatched range of physical and chemical properties) may be attributed to the many thousands of combinatorially possible structure types, in which each building block can itself adopt a range of potential isomers. Furthermore, the development of the POM chemistry has led to the realization that the isolated species could act as a set of transferable building blocks that can be reliably utilized in the formation of new materials. While these key features have been exploited frequently over the last few years, the connection between the starting materials (metallic salts of tungsten, molybdenum *etc.*), the intermediate metal-oxide building blocks, the architecture of the isolable POM-based compounds and finally the potential emergent property of the material constructed by the POM clusters has gradually became apparent. As a result, it appears to be vital that a new approach is adopted to enable control over structure, engineer properties, and develop POM-based chemical systems to achieve a high degree of designed functionality. To do this we need to understand how to 'dial-up' and direct the assembly of the desired building block libraries formed under the utilized experimental conditions. Recent in depth investigations are leading to the discovery of specific building

De-Liang Long

De-Liang Long was born in Hunan, China. He obtained his BSc and MSc degrees in chemistry from Wuhan University and PhD degree from Nanjing University (1996) in China. He was appointed as Lecturer in Hubei University (1989) and Research Assistant Professor in Fujian Institute of Research on the Structure of Matter, Chinese Academy of Sciences (1996), where he was promoted to Associate Professor (1998). In 1999 he was awarded the Royal Society KC Wong Fellowship and moved to the UK working with Professor Martin Schröder at the University of Nottingham. He joined the Cronin group in 2002. He is currently a senior research fellow (Reader Level) in Inorganic Chemistry at the University of Glasgow, and is the deputy group leader of the Cronin group. His research interests are in polyoxometalates, inorganic synthesis, coordination chemistry, cluster based materials and chemical crystallography.

Leroy Cronin

Lee Cronin is the Gardiner Professor of Chemistry at the School of Chemistry, University of Glasgow. Lee was an undergraduate and DPhil student at the University of York, research fellow at the University of Edinburgh and an Alexander von Humbolt Research Fellow at the University of Bielefeld. From 2000 to 2002 he was a lecturer at the University of Birmingham, and moved to the University of Glasgow in 2002. In 2006 he was promoted to Professor. In 2011 he was awarded the RSC Bob Hay Lectureship and 2012 the RSC Corday Morgan Medal and Prize. The work of Cronin and his research group spans a range of fields with creative studies over the entire discipline of chemistry with some focus in the field of inorganic chemistry, specifically the self-assembly and self-organization of inorganic molecules and the engineering of complex systems leading to the emergence of system-level behaviours.

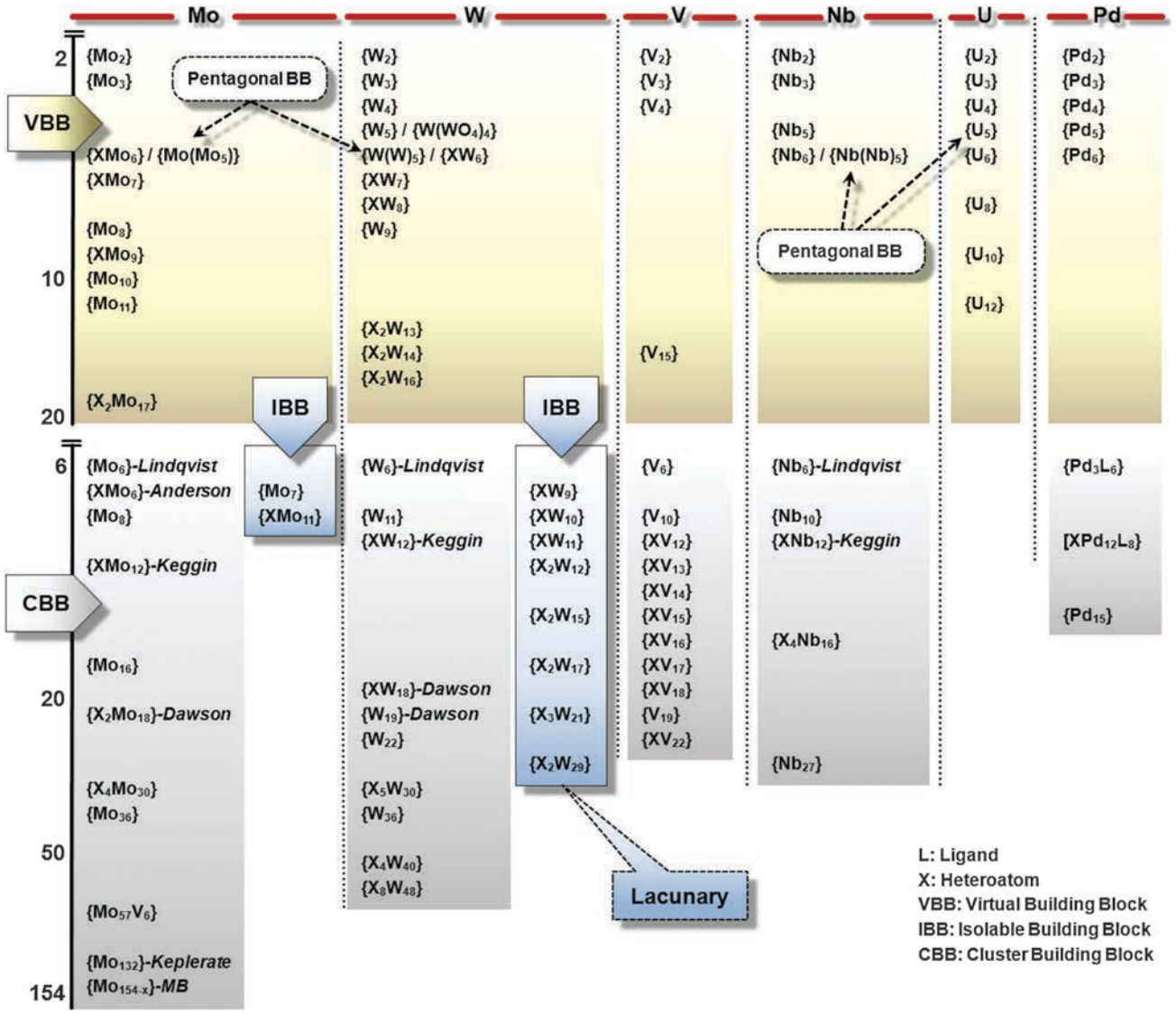

Fig. 1 Building block nuclearity using a classification based on the virtual building blocks (VBB), the isolable (IBB) and the parent-cluster-based building blocks (PCBB). The IBB have been isolated as stable clusters and are mainly lacunary tungsten-based species: lacunary Keggin (W_9X, $W_{10}X$, $W_{11}X$) and lacunary Dawson ($W_{(18-z)}X_2$). The virtual building blocks (VBBs) have not been isolated as clusters to date, but can be considered as building blocks for high-nuclearity POMs. These are: M_5 (one-metal lacunary Lindqvist; M = W, V, Nb), $W_{12}P_2$ (hexavacant lacunary Dawson), and $M(M_5)$ (pentagonal building blocks; M = Mo, W and Nb). The PCBBs are an increasingly important subset as we are learning how to control the linking of these clusters.

blocks that are used intentionally or unintentionally for the construction of POM clusters, Fig. 1, and these may provide a key engineering blue-print for the controlled assembly of new architectures. In general there are three types of building block used in POM chemistry: (1) Virtual Building Blocks (VBBs). These conserved structural units found in many cluster types, but never themselves isolated. However, since the synthesis of the clusters containing the VBBs is becoming known it should be possible to 'intercept' these units by establishing the common synthetic aspects in solution and aiming specifically for these; (2) Isolable Building Blocks (IBBs). These building blocks have well defined synthetic procedures and can be reliably synthesized; (3) Parent Cluster Based Building Blocks (PCBBs). These are clusters that can themselves be linked together using additional linking units, or by modification of the cluster itself.

3. Current trends in POM cluster design

3.1 Classic POM synthesis

Polyoxometalates (POMs) represent a unique and diverse family of compounds with numerous members derived from a huge parameter space which lies within the boundaries defined between the monomeric and low nuclearity molecular metal-oxide species and the bulk solid-state metal-oxides. The incorporation of heteroatoms, heterometallic centres, lacunary building blocks, cations and organic ligands have a profound effect on the self-assembly process and consequently the overall architecture. The architectural design principles used up until recently were based mainly on a fine balance of empirical observation and serendipity. In most cases, the utilized experimental procedures for producing POM based clusters involves

acidification of a solution of the chosen metallic salts, usually molybdates, tungstates or vanadates,[7] followed by a condensation process which involves the interaction of multiple building block libraries leading to the formation of a great variety of POM clusters. Traditionally the synthesis of the POM cluster takes place in aqueous media and involves routine procedures requiring a small number or even just one step ('one-pot' synthetic approach) with many variables as discussed above.[8,11] Recently, chemists are making efforts to re-evaluate their synthetic methodologies and adopt novel approaches which will lead to the designed synthesis of unique architectures (trapping of functional metallic cores, molecular nanoparticles, site specific activity) and potentially the emergence of novel properties (dynamic molecular organization, controlled oscillatory nano-devices, autocatalytic features) which are discussed below in detail.

3.2 Stabilization and entrapment of functional metallic cores

Many new compounds have been constructed from lacunary building units derived from polyoxotungstate species, which have been increasingly used as rigid inorganic ligands in order to stabilize multinuclear metallic cores that could significantly alter the overall functionality of the isolated material.[12] For example, our group demonstrated successfully the stabilization of a multinuclear $\{Fe_{12}(OH)_{18}\}$ core, utilizing the tirvacant polyanion $\{\alpha\text{-}P_2W_{15}O_{56}\}$ which forms an inorganic tetrameric cluster $[KFe_{12}(OH)_{18}(\alpha\text{-}1,2,3\text{-}P_2W_{15}O_{56})_4]^{29-}$.[13] Recently, a novel planar $\{Mn_{19}\}$ magnetic cluster $[Mn_{19}(OH)_{12}(SiW_{10}O_{37})_6]^{34-}$ have been isolated by Kortz *et al.* adopting a similar approach and utilization of the Keggin tungstosilicate lacunary fragment instead.[14] The planar $\{Mn_{19}(OH)_{12}\}$ core is incorporated in the centre of six $\{SiW_{10}\}$ fragments. Lately, we developed this field further by combining the stabilization effect offered from the lacunary fragments and oxidation of the manganese centres (Mn^{II} to Mn^{III}), and reported an unusual Mn mixed-valence architecture with the formula: $[Mn^{III}{}_2Mn^{II}{}_4(\mu_3\text{-}O)_2(H_2O)_4(B\text{-}\beta\text{-}SiW_8O_{31})(B\text{-}\beta\text{-}SiW_9O_{34})(\gamma\text{-}SiW_{10}O_{36})]^{18-}$.[15] The *in situ* isomerization and partial re-organization of the starting lacunary $\{\gamma\text{-}SiW_{10}O_{36}\}$ species to $\{B\text{-}\beta\text{-}SiW_8O_{31}\}$ and $\{B\text{-}\beta\text{-}SiW_9O_{34}\}$ units led to the entrapment of a mixed-valence $\{Mn_5O_6\}$ cubane core, which is structurally relevant to the oxygen evolving centre of the biological photosystem II (PSII) (Fig. 2).[16] These results demonstrate the vast possibilities and potential for the preparation of the many known multinuclear magnetic cores embedded within a POM framework which can be finely tuned and magnetically isolated altering their overall functionality. Further, the $\{\gamma\text{-}SiW_{10}O_{36}\}$, and $\{B\text{-}\beta\text{-}SiW_9O_{34}\}$ are good examples of IBBs whereas $\{B\text{-}\beta\text{-}SiW_8O_{31}\}$ is an example of a VBB.

3.3 Construction of high nuclearity nano-clusters

Synthesizing POM based nano-sized molecules is an attractive topic in POM chemistry.[17] The lacunary POM species such as $\{As_2W_{19}\}$ have been routinely used as anionic precursors while cations with high coordination number such as lanthanide ions were traditionally used as linkers.[18] Recently, Boskovic *et al.* further expanded this field by reporting the first terbium

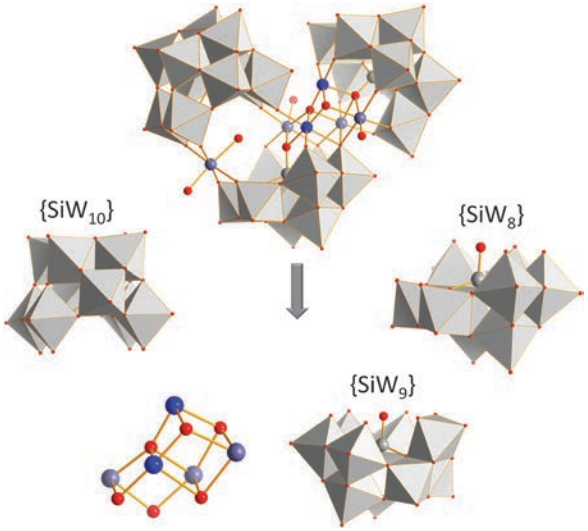

Fig. 2 Polyhedral/ball-and-stick representation of the $[Mn^{III}{}_2Mn^{II}{}_4(\mu_3\text{-}O)_2(H_2O)_4(B\text{-}\beta\text{-}SiW_8O_{31})(B\text{-}\beta\text{-}SiW_9O_{34})\text{-}(\gamma\text{-}SiW_{10}O_{36})]^{18-}$ anion, showing the three inequivalent silicotungstate Keggin fragments $\{SiW_8\}$, $\{SiW_9\}$, and $\{SiW_{10}\}$ and the $\{Mn_4O_4\}$ cubane core with an appended "pendant" Mn ion very similar to that found in the structure of photosystem II. Colour code: WO_6, grey polyhedral; Mn^{III}, blue spheres; Mn^{II}, blue-gray spheres; Si, gray spheres; and O, red spheres. Counter ions and solvent molecules have been omitted for clarity.

polyoxometalate organic complexes $[Tb_8(pic)_6(H_2O)_{22}(B\text{-}\beta\text{-}AsW_8O_{30})_4(WO_2(pic))_6]^{12-}$ (pic = 2-picolinate). The photo physical properties of this complex has revealed the importance of the smaller Tb–O–W angles, provided by edge- rather than corner-sharing connectivity, in limiting the luminescence quenching of the organic ligand-sensitized terbium centres by the POM ligands.[19] Also, the discovery of the $[\{\alpha\text{-}P_2W_{15}O_{56}\}_6\text{-}\{Ce_3Mn_2O_4(OH)_2\}_3(OH)_2(H_2O)_2(PO_4)]^{47-}$ cluster demonstrated that addition of an inorganic template anion such as $PO_4{}^{3-}$ could promote the formation of gigantic clusters.[20] The self-assembly process is promoted by the coordinatively unsaturated ("coordination number residuum") or labile binding sites, a prerequisite for further cluster aggregation. Furthermore, utilization of small templates is possible to give rise to the formation of increasingly sophisticated POM-based secondary building units and reactive aggregates. Based on this observation, it was realized that the role of small inorganic anions is more important than previously thought. However, the largest polyanion cluster isolated so far, $[Mn^{III}{}_{40}P_{32}W^{VI}{}_{224}O_{888}]^{144-}$ ($\{Mn_{40}W_{224}\}$), is not linked from lanthanide ions but only Mn^{III} precursors and the hexavacant phosphotungstate $[a\text{-}H_2P_2W_{12}O_{48}]^{12-}$ ($\{P_2W_{12}\}$); this is an example of a IBB.[21] The structure of $\{Mn_{40}W_{224}\}$ shows how different archetypal building blocks can be assembled *via* a network of Mn–O═W bridges (Fig. 3) into an unprecedented architecture. The core of the architecture is based on the intact $\{P_8W_{48}\}$ cluster unit (another example of a PCBB as shown in Fig. 1), which acts as scaffold for the organization of the remaining building blocks giving rise to the final structure. It is worth noting, that this synthetic approach appears to be transferrable and can be extrapolated to a wide range of other POM architectures in principle; this extension is important since it demonstrates the

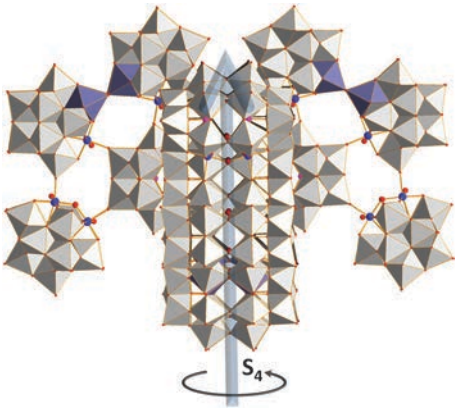

Fig. 3 Polyhedral representation of $[Mn^{III}_{40}P_{32}W^{VI}_{224}O_{888}]^{144-}$ shows all of the fragments are joined together through Mn^{III}–O═W bridges. The entire cluster adopts an idealised S_4 symmetry, with the principal axis coinciding with the four fold axis of the central $\{P_8W_{48}\}$ wheel. The WO_6 units are shown in gray polyhedra and the W/Mn disordered positions are blue gray polyhedra. Counter ions and solvent molecules have been omitted for clarity. Colour code: Mn^{III}, blue spheres; P, pink spheres; O, red spheres.

potential in using a cluster-built-on-cluster design approach to expand the size of the POM clusters way beyond the current state of the art.

3.4 Incorporation of active sites

Another advantage that derives from the unique structural features of POMs is their role as stabilizing ligands for redox active high valance metallic fragments, see Fig. 4.

For example Mizuno *et al.* has developed a synthetic methodology based on the incorporation of the catalytic active M–OH–M (M = W, Zn, or V) units in POM-based lacunary building blocks such as $\{\gamma\text{-}SiW_{10}\}$.[22] The isolation of these protonated, organic soluble clusters by controlling the reactivities of POMs using different counter cations has opened a new research avenue for POM species in catalysis.[23] Recently, the heterolytic dissociation of water at the atomic level using the $[\gamma\text{-}SiV_2W_{10}O_{39}]^{4-}$ polyanion as a catalyst (Fig. 4a) was reported. The unusual four-coordinated *syn*-linear (μ-oxo)-divanadium core $\{V_2O_3\}$ attached on the cluster, can be transformed to the five-coordinated bis(μ-hydroxo)-divanadium core $\{V_2O_2(OH)_2\}$ as confirmed by X-ray diffraction studies.[24] It is worth noting that Proust *et al.* have reported the syntheses of a few other high valance metal–nitrido POMs such as $[(Ru^{VI}{\equiv}N)_2(SiW_{10}O_{38})]^{6-}$ (Fig. 4b) by either photo oxidation of the metal–azido precursor or ligand exchanging of the metal–nitrido complex. Recent experimental and theoretical evidence demonstrated the influence of POM-based ligands on the reactivity of high-valence metal nitrido units.[25–27] The $[PW_{11}O_{39}Ru^{VI}N]^{4-}$ anion is particularly reactive and the related TBA salt reacts with triphenylphosphine to generate the first POM-based ruthenium–phosphiniminato derivative: $[PW_{11}O_{39}\{RuNPPh_3\}]^{3-}$. The cleavage of the ruthenium–nitrogen bond and the concurrent formation of PPN^+ cations validate the potential use of nitrido derivatives of polyoxometalates in nitrogen–atom transfer reactions.[28]

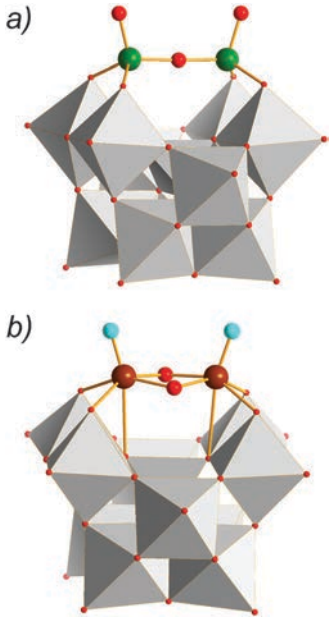

Fig. 4 Polyhedral representation of polyoxoanions with 'active cites' (a) $[\gamma\text{-}V^V_2O_3(SiW_{10}O_{36})]^{4-}$ and (b) $[(Ru^{VI}{\equiv}N)_2(SiW_{10}O_{38})]^{6-}$. The polyoxotungstate frameworks are shown in grey polyhedra and the active units are highlighted in ball and stick mode. The coordinated water molecules are shown as dark grey spheres. Colour code: WO_6, grey polyhedral; O, red spheres; V, green spheres; Ru, brown spheres; N, light blue spheres.

4. Novel synthetic approaches

The discovery of unique POM clusters with unprecedented structural motifs allows better understanding of the underlying chemistry and potential control of the assembly process. The new synthetic strategies for the synthesis of POM compounds have been extended in recent years from simple inorganic salts in aqueous media to the inclusion of structure directing organo-cations in mixed solvent systems (*e.g.* water/CH_3CN)[11,29] or even in pure organic solution,[30] while the synthetic precursors are no longer limited to lacunary cluster and metal salts.[31] Hydrothermal processing is another useful tool, becoming increasingly more popular and understood, specifically in the synthesis of POM based coordination polymers.[32,33] Lately, the use of ionic liquids as solvent/cation directing media for the directed assembly of POMs, is another new development which promises to offer an exciting alternative in the synthesis and design of functional POMs. Despite only a couple of reports thus far, this strategy could perhaps replace 'random' hydrothermal processing with a more rational approach since the reactions can be easily monitored and reagents added systematically during the reaction.[34,35]

4.1 "Bottom-up" meets "top-down" assembly

Recently we reported the synthesis and structure determination of a nanoscale phosphotungstate, $[P_4W_{52}O_{178}]^{24-}$, the largest phosphotungstate heteropolyanion reported, and its pH-controlled decomposition into smaller fragments following a "reverse-assembly" approach, to $[P_3W_{39}O_{134}]^{19-}$. This work demonstrates that the controlled fragmentation of large POM clusters is possible, leading to the formation of new

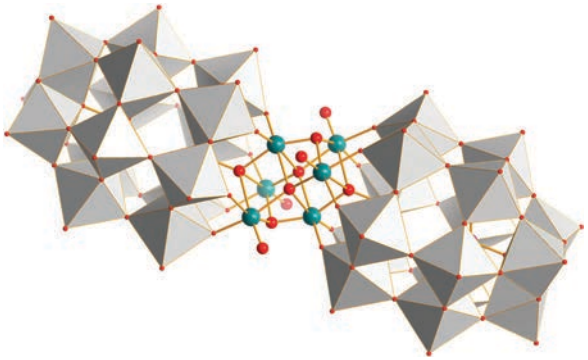

Fig. 5 Polyhedral representations of the $[P_4V_6W_{30}O_{120}]^{10-}$ species with double cubane core $\{V_6\}$. Colour code: WO_6, grey polyhedra; O, red spheres; V, Teal spheres. Counter ions are omitted for clarity.

cluster types. Although one can expect the disintegration of large POM clusters under unfavorable reaction conditions, a systematic study of such a cluster decomposition process leading to the isolation and characterization of end products as well as possible intermediates is quite unexpected. The expansion of this work based on the "reverse-assembly" approach could offer an opportunity to develop a new synthetic strategy based upon the assembly–disassembly paradigm of similar system.[31]

A recent example of an organically soluble vanadium substituted Wells–Dawson sandwich cluster $[P_4V_6W_{30}O_{120}]^{10-}$ incorporating a six vanadium double cubane core was reported by us using the pre-formed $\{P_2W_{15}V_3O_{62}\}$ clusters which do not degrade under the reaction conditions (Fig. 5). The tri-vanadium substituted Dawson $\{P_2W_{15}V_3O_{62}\}$ species with tetrabutylammonium (TBA) counter ions refluxed in acetonitrile to yield the overall $[P_4V_6W_{30}O_{120}]^{10-}$ sandwich. The benefit of this reaction is that there are no side products formed and the compound can be purified by simple crystallization. The vanadium atoms in this compound are readily reduced in a two-step process as has been demonstrated by electrochemistry and stopped flow UV/vis techniques whilst the final compound retains its integrity under the experimental conditions used and can receive up to four electrons with marginal structural re-arrangement. This work is very important in the field of POM chemistry as it blends elements of hybrid and traditional POM chemistry, demonstrating the advantages of combining transition metal substituted POM frameworks and organic cations.[30]

4.2 "Shrink-wrapping" and crystal engineering

From the crystal engineering point of view, one of the crucial factors that affect the formation of a particular POM species is directly related to the crystallisation process itself. This variable is brought into focus when one realises that the POM compounds are poly-anions and obviously cannot exist without the charge balancing provided by the associated cations, which often define the cationic environment in which the anion is assembled. This logically leads to the obvious idea that the cations should be able to direct and control the formation of a specific moiety, see Fig. 6, perhaps even *during the crystallization process*.[36] Since the inherent properties of the cations

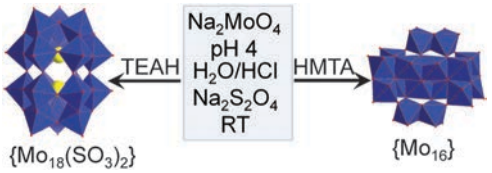

Fig. 6 A demonstration of the cationic effect on POM formation. Colour code: Mo, blue spheres; O, red spheres; S, yellow spheres. The $\{SO_3\}$ moieties are shown in a space filling and MoO_6 in blue polyhedra.

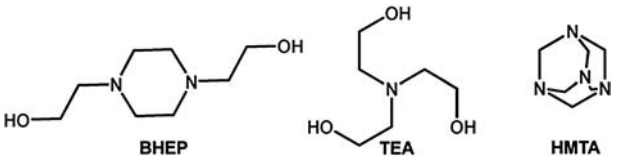

Scheme 1 Representative set of "shrink-wrapping" cationic precursors used in our studies.

such as size, charge, symmetry, solubility *etc.* are found to modulate the reactivity of the POM building blocks, these cations can affect the nature of the obtained final product.[11,37,38] Also, the distribution of cations, anionic POM building units and their possible combinations in the reaction mixture and finally into a specific crystal lattice arrangement, highlights the vast number of possibilities and the potential for novel discoveries.

Using a crystal facilitated assembly/engineering approach for the construction of novel POM species, there are two important aims that needs to be taken into consideration: (a) the discovery of novel POM building blocks and (b) to direct their self-assembly in a controlled fashion to form novel architectures with potential useful functionality.[8] A simple strategy in order to achieve these targets, is based on the metathesis of the cations to bulky organic amine cations as counter-ions during the synthetic procedure.[39–41] The use of bulky cations prevents the rapid aggregation of POM-based synthons into clusters of stable and uniform spherical topology. Also such cations together with other linker units are found to be capable of stabilizing intermediate reactive secondary building units and directing their self-assembly into novel archetypes. Recently we introduced the term "shrink wrapping" in order to describe this approach.[42–44] More specifically, the use of organic amines such as hexamethylene tetramine (HMTA), triethanol amine (TEA), *N*,*N*-bis-(2-hydroxyethyl)-piperazine (BHEP), morpholine *etc.* which are capable of acting as cations, as well as ligands, buffers and even as redox reagents in some cases, see Scheme 1, were proven to be useful tools for directing the self-assembly process. Extensive use of the above amines gave us the opportunity to isolate a number of discrete iso- and heteropolyoxometalate clusters as well as many extended architectures using this simple but efficient concept.

4.3 Hydrothermal and ionothermal synthesis

Besides the conventional solution synthesis, solvothermal and ionothermal synthesis are two other methods that have been used more often lately for the isolation of novel POM-based compounds; indeed the hydrothermal technique is used to a large degree and can produce known clusters as unknown

compounds which are new only by virtue of the use of different salt combinations. The use of water or organic solvents (*e.g.* acetonitrile, methanol and pyridine) limits the reaction temperature during the course of conventional synthesis. Due to the above limitations, the use of Teflon auto-claves during the solvothermal process gives the opportunity to reach higher temperatures at higher pressures for the same reaction mixture. Under these conditions, metastable or intermediate phases (VBBs) can be formed which normally lead to kinetically controlled products, such as the "basket-shaped" cluster $[P_6Mo_{18}O_{73}]^{11-}$.[45] However, solvothermal methods are based on the generation of significant autogenous pressure when the reaction mixture is heated in a sealed container which engenders an intrinsic weakness: the general reproducibility of the reactions requires perfect control of reaction parameters. Additionally, the reaction temperature is still limited due to safety concerns. On the other hand, the ionothermal synthesis which was recently employed by Wang *et al.*, Pakhomova *et al.* and others, has started to be used widely by POM chemists.[35,46,47] During this approach, an ionic liquid acts as a solvent, potential template, and structure-directing agent in a similar fashion to the "shrink wrapping" strategy,[11] while at the same time much higher temperatures can be applied to the system. Altering the anionic component of the ionic liquid can result in the selective synthesis of different POMs by influencing their self-assembly. For example, a high-nuclearity transition-metal-substituted polyoxometalate, has been reported recently which is composed of three $[a\text{-}SiW_9O_{34}]^{10-}$ Keggin moieties connected *via* a $\{WFe_9\}$ cluster core (Fig. 7).[35] Ionic liquids also have numerous properties, such as high chemical and thermal stability, a wide working temperature range, low toxicity and little or no volatility, which make them ideal solvents for organic and inorganic synthesis. Furthermore, their ionic character makes them ideal polar solvents suitable for the dissolution of many different types of inorganic precursors.

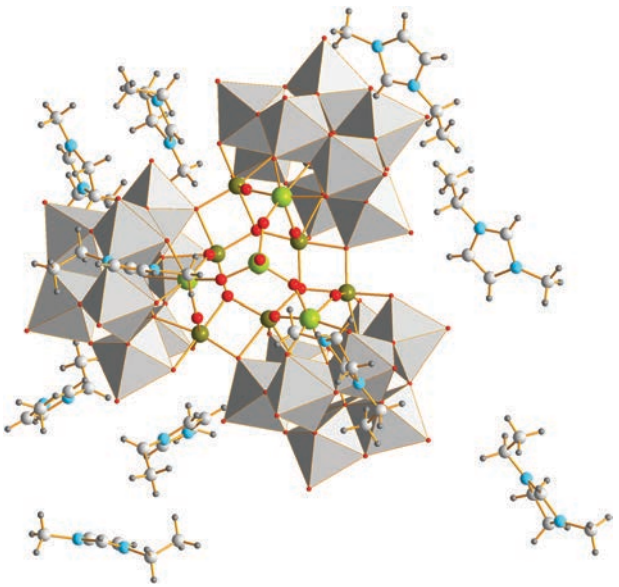

Fig. 7 Representation of the $[WFe_9(OH)_6O_7(H_2O)(SiW_9O_{34})_3]^{17-}$ cluster wrapped with 1-ethyl-3-methylimidazolium cations. The polyoxotungstate framework is shown in polyhedra and the metallic core is highlighted in ball and stick mode. Colour code: WO_6, grey polyhedra; Fe, dark yellow spheres; O, red spheres; W/Fe, light green spheres; C, brown spheres; N, light blue spheres; H, gray dots).

4.4 Assembly of POMs in flow systems

Recently we pioneered the use of a flow reactor system approach to both explore the mechanism, and the synthesis of complex polyoxometalate clusters. For example, by using the flow system we were able to generate a stationary kinetic state of the 'intermediate' molybdenum-blue (MB) wheel, filled with a $\{Mo_{36}\}$ guest to give a host–guest complex.[48] The MB host–guest complex has the form $Na_{22}\{[Mo^{VI}_{36}O_{112}(H_2O)_{16}]\subset[Mo^{VI}_{130}Mo^{V}_{20}O_{442}(OH)_{10}(H_2O)_{61}]\}\cdot 180H_2O \equiv \{Mo_{36}\}\subset\{Mo_{150}\}$. Carrying out the reaction under controlled continuous flow conditions enabled selection for the generation of $\{Mo_{36}\}\subset\{Mo_{150}\}$ as the major product, and allowed the reproducible isolation of this host–guest complex in good yield, as opposed to the traditional "one-pot" batch synthesis which typically leads to crystallization of the $\{Mo_{154-x}\}$ species (Fig. 8).[48] Structural and spectroscopic studies identified the $\{Mo_{36}\}\subset\{Mo_{150}\}$ compound as the intermediate in the synthesis of MB wheels. It is interesting to note that, compared to the archetypal 28 electron reduced 'empty' $\{Mo_{154}\}$ wheel, the $\{Mo_{150}\}$ is only 20 electron reduced. This is of crucial importance since further reduction of the wheel results in the expulsion of the $\{Mo_{36}\}$ guest indicating why this was not observed before reproducibly. Also, further experiments showed an increase in the yield and the formation rate of the $\{Mo_{154-x}\}$ wheels by deliberate addition of preformed $\{Mo_{36}\}$ to the reaction mixture. Dynamic light scattering (DLS) was also used to corroborate the mechanism of formation of the MB wheels through observation of the individual cluster species in solution. DLS measurement of the reaction mixtures, from which $\{Mo_{36}\}$ and $\{Mo_{150}\}$ crystallized, gave particle size distribution curves averaging 1.9 and 3.9 nm respectively. The above approach allowed the use of size as a possible distinguishing feature of these key species in the reduced acidified molybdate solutions and direct observation of the molecular evolution of the available synthons to MB wheels.[49]

Although the qualitative data obtained does not allow comprehensive kinetic studies at this stage, it brings us one

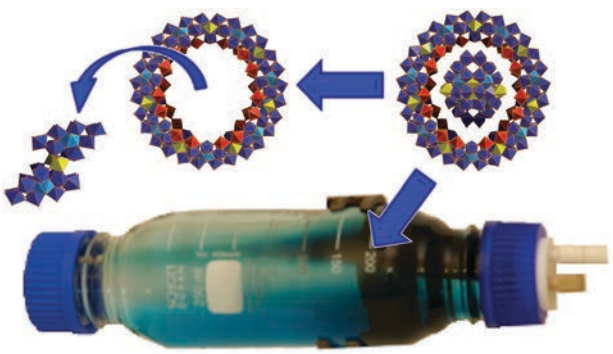

Fig. 8 Representation of the flow system from which the $\{[Mo^{VI}_{36}O_{112}(H_2O)_{16}]\subset[Mo^{VI}_{130}Mo^{V}_{20}O_{442}(OH)_{10}(H_2O)_{61}]\}^{22-}$ anion crystallises while further reduction causes the ejection of the $[Mo^{VI}_{36}O_{112}(H_2O)_{16}]^{8-}$ template, to give the empty wheel, $[Mo^{VI}_{122}Mo^{V}_{28}O_{442}(OH)_{10}(H_2O)_{66}]^{14-}$.

step closer to understanding the formation of complicated systems like the MBs in solution. Using these techniques to follow the assembly of other self-assembled chemical systems in solution will open the door to further understanding and finally control of such complex self-assembly processes. The characterization of the "bottom-up" designed nanosized species in solution will also overcome the problems associated with product crystallization and isolation and will ultimately unveil the true potential of solution-processable nanosized metal oxides to be exploited in the manufacture of novel materials and molecular devices with engineered functionality.

4.5 Novel templates: XO_3-templated POMs

Anions of the general formula $\{X^{IV}O_3\}$ have been used extensively as templates in order to build lacunary fragments which can be used as secondary building units for the construction of large architectures.[50] However, we demonstrated that the assembly of the POM building blocks is far more complicated and larger POM clusters can be obtained by utilizing pyramidal heteroanions as templates as well as linkers under "one-pot" conditions. For example, a series of new high nuclearity polyoxotungstates clusters $\{W_{43}Se_3\}$, $\{W_{77}Se_5\}$, $\{W_{63}Se_6\}$ and $\{W_{100}Se_{16}\}$ have been synthesized using the SeO_3^{2-} anion inorganic ligand. Interestingly, this family of polytungstate clusters is the first that incorporate building units with pentagonal geometry which have been observed in molybdenum blue systems and known for their potential to form spherical and toroidal clusters.[51] Such clusters have a great potential in the construction of new nanomaterials with many applications and the ability to engineer large low symmetry systems is also of fundamental interest. In a similar manner, we reported recently the isolation of the pentagonal $\{WO_7\}$-based giant $[H_{34}W_{119}Se_8Fe_2O_{420}]^{54-}$ polyoxotungstate cluster (Fig. 9). The Se-based units $\{Se_2W_{29}\}$ form the "branches" and a Fe-based core links the units together. Overall the cluster has a unique saddle shape and nanoscale size, representing the biggest polyoxotungstate framework containing pentagonal units so far. Furthermore, the flexible

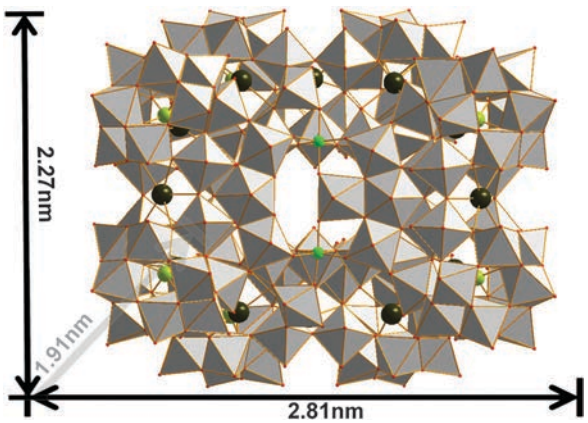

Fig. 9 Polyhedral and ball-and-stick representation of $[H_{34}W_{119}Se_8Fe_2O_{420}]^{54-}$. The polyoxotungstate framework is shown in polyhedra and the central Fe centres are highlighted in ball and stick mode. Colour code: WO_6, gray polyhedra; Fe, Green spheres; O, red spheres; K, dark green spheres). Counter ions and solvent molecules are omitted for clarity, and the cluster measures 2.8 nm at its widest point.

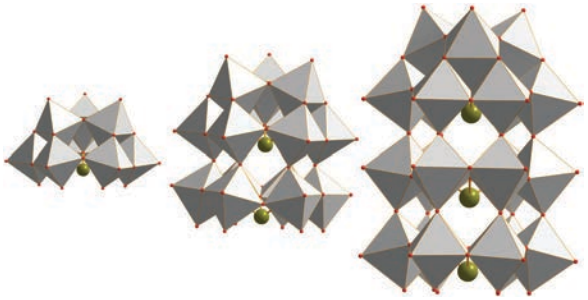

Fig. 10 New members of the one-, two- and three-layered Te^{IV} containing HPOM "pagoda" building blocks. The polyoxotungstate frameworks are shown in polyhedra and the central TeO_3^{2-} are highlighted in ball and stick mode. Colour code: WO_6, grey polyhedra; Te, dark yellow spheres; O, red spheres.

assembly of the pentagonal $\{WO_7\}$ moieties effectively gives rise to the formation of the unique $\{W(W_5)\}$ building units and the Fe-substituted pentagonal species $\{W(W_4Fe)\}$, which direct the assembly of this gigantic 2.8 nm solution-stable cluster.[52]

Further systematic studies on the TeO_3^{2-} based POMs have shown that the template give rise to high nuclearity clusters in a similar manner. Using a time-dependent synthetic approach, the construction of a new class of tungsten based macrocyclic structures, $[W_{28}Te_8O_{112}]^{24-}$, $[W_{28}Te_9O_{115}]^{26-}$ and $[W_{28}Te_{10}O_{118}]^{28-}$ have been reported.[53] Isolation of these architectures is facilitated by the tellurite anions, which act as templates within the structural building units as well as bridges between them. Additionally, the tellurite anions act as pendant ligands which subsequently control the inter-cluster aggregation, thereby defining a new architectural principle in the assembly of polyoxotungstate clusters. A similar behaviour has been observed in the case of mixed-metal, mixed-valence polyoxomolybdenum/vanadium–tellurite clusters such as $[Mo^{VI}{}_{12}V^{V}{}_{8}V^{IV}{}_{4}Te^{IV}O_{69}(Te^{IV}O_3)_2]^{10-}$ where the cooperative effect of the counter ion along with the size of the hetero-ion was demonstrated, allowing the discovery and isolation of this novel family of POMs.[54]

Moreover, we recently reported the discovery of a "layered" family of tungstatotellurite compounds which show unique layered structures built from a series of non-conventional Te^{IV}-containing POM building blocks, *i.e.* $[TeW_9O_{33}]^{8-}$, $[Te_2W_{15}O_{54}]^{10-}$, and $[Te_3W_{21}O_{75}]^{12-}$ utilizing the "shrink wrapping" strategy (Fig. 10). These molecules incorporate a new family of building blocks which consist of a $\{W_3\}$ top unit and n layers of $\{TeW_6\}$ (n = 0,1,2). There is a principal axis of TeO_3^{2-} on which the lone pair of electrons is located, with all lone pairs orientated towards the open end of the cluster. The possibility to access "layered" clusters opens the door to more extended systems, whilst the linking of such units allows the design of nanostructured clusters whose architecture is controlled by the presence of appropriate cations, as demonstrated in the case of the tetrameric cluster $\{Te_8W_{64}O_{224}\}$.[55]

4.6 Novel templates: XO_6-templated POMs

Another case of non-conventional heteroanions is the XO_6 type which is rarely used for the construction of nano sized POMs. The majority of the structures reported so far are based on the Anderson archetype.[56] Nevertheless, we have recently demonstrated the first example of non-classic Dawson

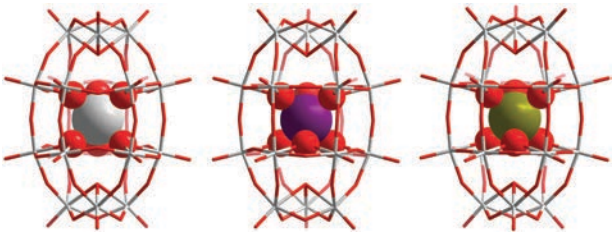

Fig. 11 Representation of the non-classical Wells–Dawson $\{W_{18}X\}$ type POMs. The $\{W_{18}\}$ cages are shown in wireframe and the central $\{XO_6\}$ group is represented in space-filling mode. Left: α-$[W_{18}O_{56}(WO_6)]^{10-}$. Middle: β*-$[W_{18}O_{56}(IO_6)]^{9-}$. Right: γ*-$[W_{18}O_{56}(XO_6)]^{10-}$ X = W^{VI} and Te^{VI}. Colour code: W, grey; O, red; Te, dark green; I, violet.

POM $[H_4W_{19}O_{62}]^{6-}$.[42] The cluster consists of the typical $\{W_{18}O_{54}\}$ cage framework as in the classical Dawson structure ($[W_{18}O_{54}(XO_4)_2]^{y-}$, X = P, S) but the two tetrahedral XO_4^{n-} heteroanions are replaced by a either an octahedral or a trigonal-prismatic WO_6^{6-} anion and two protonated μ_3-oxido ligands. The stabilization of the $\{WO_6\}$ moiety in a trigonal prismatic coordination environment was unprecedented in polyoxotungstate chemistry. Furthermore we showed that the metal- and heterometal-based octahedra allow the controlled formation of Dawson type clusters utilizing $\{MO_6\}$ or $\{XO_6\}$ units as templates (Fig. 11). Following the same approach and based on the analogy of the tungstatoperiodate and tungstatotellurate compounds, $[H_nW_{18}O_{56}(XO_6)]^{m-}$ (X = I^{VI} or Te^{VI}), we reported the discovery of Dawson capsules which incorporate either high-valent $I^{VII}O_6$ or the $Te^{VI}O_6$.[57,58] The $[H_3W_{18}O_{56}(IO_6)]^{6-}$ is the first example of a β*-Dawson isomer and its electrochemical, catalytic and DFT studies show significant differences compared with those observed for the conventional Dawson-type polyoxotungstates.[59] Further, the selective reduction of the γ*-$[H_3W_{18}O_{56}(TeO_6)]^{7-}$ yielded $[H_3W_{18}Te^{IV}O_{60}]^{5-}$, which resulted in both electronic and structural reorganizations of the Te-based ion within the cluster shell. Control of the solution's pH allowed us to isolate a nanosized high nuclearity POM polytungstate $[H_{10}W_{58}Te^{VI}_2O_{198}]^{26-}$ anion without using additional electrophilic linkers.

5. New POM networks

Extended modular frameworks that incorporate inorganic building blocks represent a promising new field of research strand where "active sites" can be engineered to respond to guest inclusion. These functionalized modular frameworks can initiate highly specific chemical reactions altering the overall behaviour of the material and may even be used to facilitate directed chemical reactions similar to those found in enzymatic systems. As such, the design and isolation of these compounds defines a new research direction which bridges the gap between coordination compounds, metal–organic frameworks and solid-state oxides.

5.1 'Pure' metal oxide frameworks

Recently, we reported the directed assembly of the first 3D POM-based framework, $[(C_4H_{10}NO)_{40}(W_{72}Mn_{12}O_{268}X_7)]_n$ (X = Si or Ge) which is based on the substituted Keggin-type POM building blocks and yields a material that can undergo a reversible redox process that involves the simultaneous inclusion of the redox reagent with a concerted and spatially ordered redox change of the framework (Fig. 12).[29] Furthermore, we have demonstrated that it is possible to construct framework architectures that undergo controlled reversible single-crystal to single-crystal (SC–SC) redox transformations, where the kinetics of the processes is controlled by the redox agent and the heteroatom embedded within the Keggin moieties.[60] This work showed that it is possible to modify the overall structure following a redox-based "post-assembly" modification. This opens up a plethora of applications whereby redox-tunable frameworks such as those discussed here could be applied as sensors or catalysts. Extending this piece of work, another two new members $\{(C_4H_{10}NO)_{46}[W_{72}Co^{II}_{12}X_7(OH)_6O_{262}]\}_n$ (X = Si or Ge) of the "Keggin Net" family were isolated. The introduction of the cobalt heterometal has altered the redox activity of this family of compounds. The Co^{II} bridging metal centres can be oxidized to less stable Co^{III} analogue in a reversible SC–SC transformation in which the framework integrity of the material is completely retained. Furthermore, the concept of molecular alloys has been realized for the first time in the context of 3D inorganic frameworks and is demonstrated by a series of linked mixed Co/Mn polyoxometalate networks, thus opening up another route to discover new electronically interesting materials with emergent physical properties.[61] Further, a similar synthetic strategy which employs

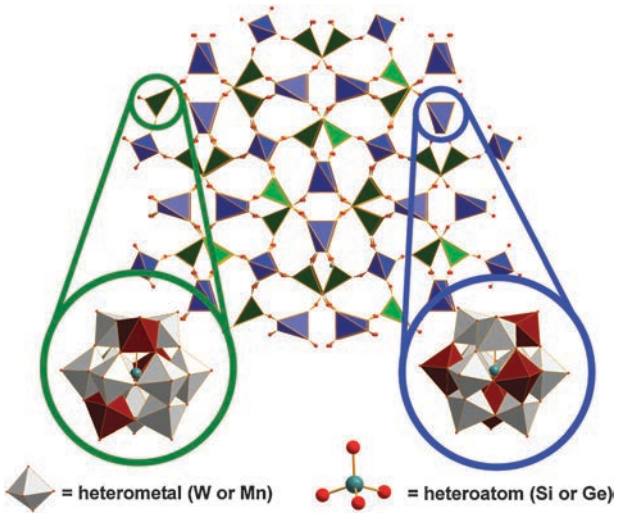

Fig. 12 Representation of the "Keggin-net" structure $(C_4H_{10}NO)_m[W_{72}M^{II/III}_{12}X_7O_{268}]$ (where M = Co^{II} or Mn^{III}; X = Si or Ge) constructed from two types of transition-metal-substituted a-Keggin clusters: 4-connected (blue tetrahedra) and 3-connected (green triangles). The overall structure is represented by linked 3- and 4-connected polyhedra with the oxygen linkers (red spheres) and the structure of the 3- and 4-connected Keggin-nodes shown in green and blue inserts, respectively. Insets: the "modular" or interchangeable components are shown as cyan polyhedra (the octahedrally coordinated heterometal centre) and teal spheres (the tetrahedrally coordinated heteroatom centre). Colour code: Heterometal (Mn or Co), dark red polyhedra; W, grey polyhedra; O, small red spheres; heteroatom (Si or Ge), teal spheres. Counterions and solvent molecules are omitted for clarity.

other metal ions (M) and heterotemplates (X) should result in the formation of a family of related materials. The combination of the structurally conserved redox switching and the ability to reform the material by repeated dissolution and recrystallization underlines its unique nature, offering a great deal of potential for investigations of this new type of functional and responsive material.

Another interesting example is the face-directed assembly of a ring-shaped macrocyclic polyoxometalate structural building unit, $[P_8W_{48}O_{184}]^{40-}$ with an integrated 1 nm pore as an 'aperture synthon', with manganese linkers yielding a vast three dimensional extended framework architecture based on a truncated cuboctahedron (Fig. 13).[62] The 1 nm-diameter entrance pores of the $\{P_8W_{48}\}$ structural building unit lead to approximately spherical 7.24 nm^3 cavities containing exchangeable alkali-metal cations that can be replaced by transition-metal ions through a cation exchange process.

Fig. 13 TOP: (a) Polyhedral representation of the face-directed assembly of the $[P_8W_{48}O_{184}]^{40-}$ molecular building unit, combined with electrophilic manganese linkers; (b) Crystal packing of $[Mn_8(H_2O)_{48}P_8W_{48}O_{184}]^{24-}$ along the crystallographic *a* axis. Colour code: WO_6, grey polyhedra; O, red spheres; Mn, blue spheres; P, pink spheres. Counterions and solvent molecules are omitted for clarity. BOTTOM: A scheme showing the assembly of the cube with the $\{W_{48}\}$ clusters each colour coded.

The whole process can be controlled either *via* electrochemical switching of the overall framework charge by manipulating the oxidation state of the manganese linker ions or by physically gating the pores with large organic cations, thus demonstrating how metal–organic framework-like structures with integrated pores and new physical properties can be designed.

5.2 Polyoxometalate-based molecular cages and POMOFs

In the rapidly developing context of hybrid framework materials or metal organic frameworks, POMs constitute ideal building blocks for targeting new multifunctional molecules. Recently, a new class of POM-based metal organic cages and POM-based MOFs (so-called POMOFs), which are built from the connection of POMs to one another through bridging organic linkers, have been demonstrated. Using POM molecular secondary building blocks as large vertexes to construct coordination cages is still a significant challenge for chemists. Schmitt *et al.* firstly studied the formation of POMs in the presence of organic arsenic and phosphoric acids and obtained several novel POM capsules where they observed that simple extension of the organic ligands affects the formation of elongated hybrid capsules.[63,64] Recently, Yang *et al.* reported another example of this type of cage, $[Ni(en)_2(H_2O)_2]_6\{Ni_6(Tris)(en)_3(BTC)_{1.5}(B\text{-}\alpha\text{-}PW_9O_{34})\}_8$ (Tris = tris(hydroxymethyl)aminomethane, en = ethylenediamine, BTC = 1,3,5-benzenetricarboxylate) (Fig. 14). The Tris ligand was successfully grafted onto the surface of a Ni_6-substituted polyoxotungstate formed *in situ* to further generate a three-connected polyoxometalate building block. The cooperative assembly of Tris functionalized three-connected building blocks and rigid BTC gave rise to a cubic polyoxometalate–organic molecular cage with high thermal and hydrothermal stability.[65]

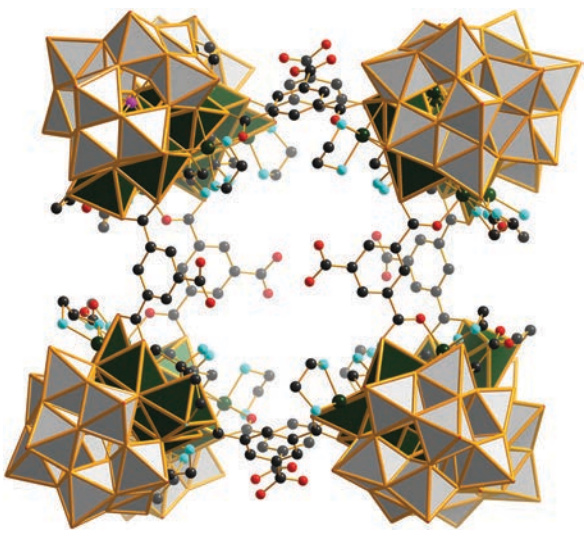

Fig. 14 Representation of the structure of the molecular cage. The POM structure $\{PW_9Ni_6\}$ is shown in polyhedral representation and the organic moieties in ball-and-stick mode. Colour code: W, grey polyhedra; Ni, dark green polyhedral; O, red spheres; N, light blue spheres; P, pink spheres; C, small black spheres. The chelated en ligands are omitted for clarity.

Moreover, a few novel 3D POMOFs materials have been reported recently.[66] Dolbecq *et al.* have developed a new family of POMOFs using ε-Keggin POMs as building blocks. This POM has the general formula $\{\varepsilon\text{-}PMo^{V}_{8}Mo^{VI}_{4}O_{40-x}(OH)_{x}M_{4}\}$ ($M = Zn^{II}$, La^{III}) and contains an ε-Keggin core capped by four M metallic ions. These Keggin entities are versatile building blocks that may be used either as anions (M = Zn, $x = 0$) or cations (M = Zn, La, $x = 3$–5). The ε-Keggin ion has a remarkable ability to successfully react with a variety of organic linkers such as bipyridine, benzenedicarboxylic acid (BDC), or imidazole (Fig. 15).[67] Specifically, the Zn-ε-Keggin possesses a tetrahedral shape in which four Zn^{II} cations are exposed in a regular tetrahedral arrangement in a fashion similar to oxygen atoms in SiO_4. As well as ditopic ligands, the grafting of the triangular 1,3,5-benzene tricarboxylate linkers (denoted trim) on this Zn-capped ε-Keggin POM, formed *in situ* under hydrothermal conditions, has generated three novel (POMOFs). $(TBA)_3[PMo^{V}_{8}Mo^{VI}_{4}O_{36}(OH)_4Zn_4][C_6H_3(COO)_3]_{4/3}$ (ε(trim)$_{4/3}$) is a 3D open-framework built of molecular Keggin units connected by trim linkers, with channels occupied by TBA counter ions. Computer simulations have been used to evaluate its relative stability in comparison with other polymorphs, showing high stability of this novel phase, which correlated with its higher density. By slightly varying the experimental conditions, POM building blocks can be further condensed and form new dimeric, or chainlike subunits leading to the isolation of modified frameworks like $(TBA)_3[PMo^{V}_{8}Mo^{VI}_{4}O_{37}(OH)_3Zn_4][C_6H_3(COO)_3]$, in which the building unit is a dimerized form of the POM. Their connection *via* trim linkers generates a 3D framework with channels also filled by TBA cations. Further, a remarkable electrocatalytic hydrogen evolution reaction was detected on these POMOF modified electrodes and this unique feature of POMOFs to allow the stabilization of electro-active POMs

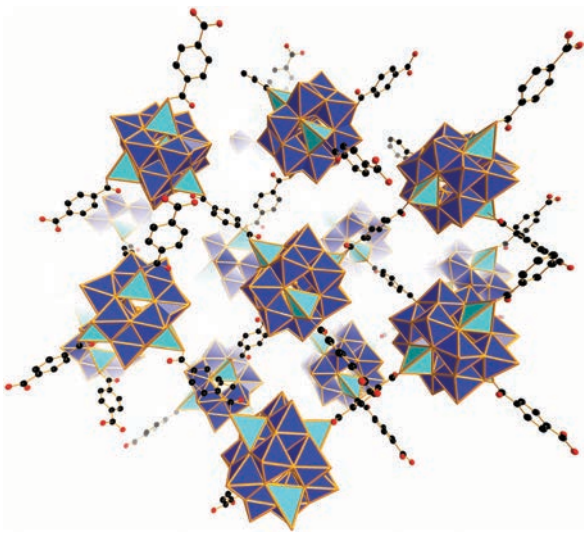

Fig. 15 Representation of the $(TBA)_3[PMo^{V}_{8}Mo^{VI}_{4}O_{36}(OH)_4Zn_4][C_6H_3(COO)_3]_{4/3}$ POMOF composite. The POM is shown in polyhedral representation and the organic ligands are represented in ball and stick mode. TBA cations and hydrogen atoms are omitted for clarity. Colour code: Mo, blue polyhedra; O, red spheres; Zn, sky blue polyhedra; C, black spheres.

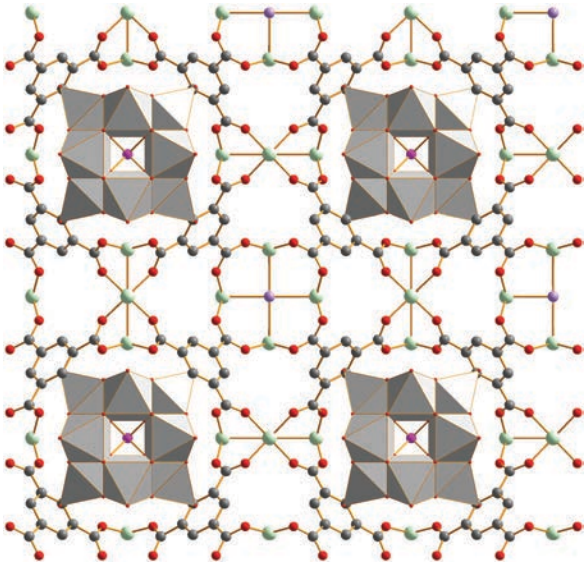

Fig. 16 Representation of the $H_3[(Cu_4Cl)_3(BTC)_8]_2[PW_{12}O_{40}]\cdot(C_4H_{12}N)_6\cdot 3H_2O$ POMOF composite. The Cu-BTC framework and Keggin polyanions are represented by ball-and-stick and polyhedral models respectively. TBA cations and hydrogen atoms are omitted for clarity. Colour code: W, Gray polyhedra; O, red spheres; Cu, light green spheres; C, black spheres; Cl, light violet spheres.

in MOF-type scaffolds opens up promising perspectives for the design of more efficient catalysts.[33]

Additionally, POMs have not only been used as vertex-linkers, but also template the channel formation of certain MOFs. Liu *et al.* isolated a series of crystalline compounds $[Cu_2(BTC)_{4/3}(H_2O)_2]_6[H_nXM_{12}O_{40}]$ X = Si, Ge, P, As; M = W, Mo) obtained using a simple one-step hydrothermal reaction between copper ions, benzentricaboxylate (BTC) and POMs.[68] In these compounds, the catalytically active Keggin polyanions were alternately arrayed as non-coordinating guests in the cuboctahedral cages of a Cu-BTC-based MOF host matrix with high stability and tolerance for thermal and acid–base conditions (Fig. 16). Further, instead of using hydrothermal methods, the stepwise approach also been employed in the synthesis of POMOFs. Wu *et al.*[69] reported the synthesis of a layered POM–Mn^{III}–metalloporphyrin based hybrid network, $\{[Cd\text{-}(DMF)_2Mn^{III}(DMF)_2TPyP]\text{-}(PW_{12}O_{40})\}_n$ (DMF = *N*,*N*-dimethylformamide; TPyP = tetrapyridylporphyrin), which is constructed by layers of POM anions and porphyrin-containing cationic nets. Briefly, the hybridization of POMs and POMOFs discussed here shows a promising approach for the design and construction of this kind of multifunctional material. By virtue of the porosity of MOF hosts and the numerous properties of POM guests, these materials are excellent candidates for the design of materials with tunable functionality.[69]

6. New metallic centres

The majority of new POM structural motifs reported every year are based on the traditional structures and metals, with only small variations and alterations. However, during the last few years this paradigm has started to move towards the

discovery/design of new compounds beyond traditional POM (based upon Mo, W, V), to oxo clusters based upon niobium, platinum, palladium *etc*., in a quest for innovative applications and the emergence of new functionalities. Here we discuss some representative examples of novel and non-conventional POM compounds reported during the last few years.

6.1 Polyoxoniobates

The assembly of polyoxoniobates has mainly focussed on isopolyniobates, *e.g*. $[Nb_6O_{19}]^{8-}$ Lindqvist ion. Nyman *et al*. reported the polyoxoniobate cluster type $[Nb_{24}O_{72}H_9]^{15-}$.[70] This cluster is constructed by two fundamental structural types; the condensed octahedral $\{Nb_6\}$ ring and an open $\{Nb_6\}$-ring which can serve as a building block for even larger clusters and extended structures.[27] We have recently discovered the largest polyoxoniobates $[HNb_{27}O_{76}]^{16-}$ and $[H_{10}Nb_{31}O_{93}(CO_3)]^{23-}$ reported so far. Interestingly, these clusters also incorporate pentagonal building units and were assembled in the presence of dibenzyldithiocarbamate, even though the actual role of the organic reagent has not been clarified (Fig. 17).[71]

Further, Casey *et al*. reported the synthesis and characterisation of a new type of POM structure $[Ti_{12}Nb_6O_{44}]^{10-}$,[72] which forms a super-octahedron. The "super-Lindqvist" cluster has 6 Nb centres located on the vertices of the octahedron and 12 Ti atoms in the middle point of each of the 12 edges. The remarkable feature is that there is a central cavity large enough to hold another Nb atom, which is empty in this particular case. Also, it may be possible to embed these clusters in titania and other oxides to produce novel materials based on the Nb-oxides. In this area it will be interesting to see if a range of new structures/processing approaches are adopted and if new physical properties for the normally inert Nb centre can be found and exploited, especially given the new pentagonal structure architectures discovered and described above.[70] One startling trend in polyoxoniobates is that their solubility in water (Cs salt most soluble, Li salt least soluble) is opposite to what is expected from the classical aqueous solubility behaviour of POMs, as first discovered with the $[Nb_6O_{19}]^{8-}$. This was recently confirmed to also be true for larger niobium POM structures. This might open up the possibility to investigate further this unexpectedly rich chemistry and the potential applications of heteropolyniobates, including ion association in solution, incorporation into functional surfaces and materials, homogeneous catalysis, and microbiological applications.[73,74]

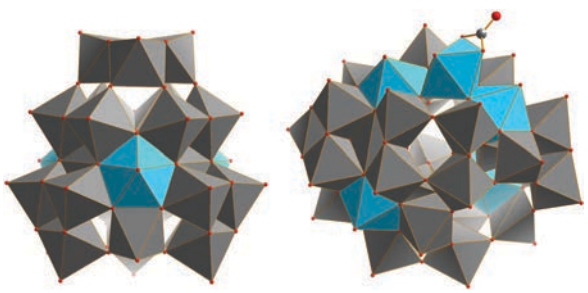

Fig. 17 Representation of the $[HNb_{27}O_{76}]^{16-}$ (left) and $[H_{10}Nb_{31}O_{93}(CO_3)]^{23-}$ (right) polyanions. The polyoxoniobates fragments are shown in polyhedra and the $\{NbO_7\}$ pentagonal building units are highlighted in light blue. Colour code: NbO_6, grey polyhedra; O, red spheres; C, black spheres.

6.2 Uranium-based POMs

Although the classification of POM clusters can be very helpful, the central paradigms are constantly being challenged as the result of new synthetic and structural developments. For instance the peroxo-uranium compounds are certainly not classical POM clusters, but exhibit certain key similarities, especially regarding their larger structures resulting from a range of linkable building units.[75] The peroxide groups bridging between uranyl ions forces the $\{U–(O_2)–U\}$ unit to bend. This bent configuration favours the formation of cage clusters, rather than polymer 1D sheets of uranyl polyhedra and a rapid self-assembly of uranyl building units into fullerene-type cage clusters was reported recently by Burns and co-workers.[76] More specifically, they isolated a complex core–shell cluster constructed by 68 uranyl peroxo polyhedra in alkaline aqueous solution under ambient conditions (Fig. 18). The cluster, which can be designated as $\{U_1 \subset U_{28} \subset U_{40}R\}$, contains a fullerene-topology cage and is built from 28 uranyl polyhedra. A ring consisting of 40 uranyl polyhedra linked into five-membered rings and 16 nitrate groups surrounds this cage cluster. Topological pentagons in the cage and ring are aligned, and their corresponding rings of uranyl bipyramids are linked through K^+ cations located between the two shells. A partially occupied U site is located at the center of the cluster but a key issue in this area is to increase the yield and explore the functionality/host guest properties of these clusters.[76]

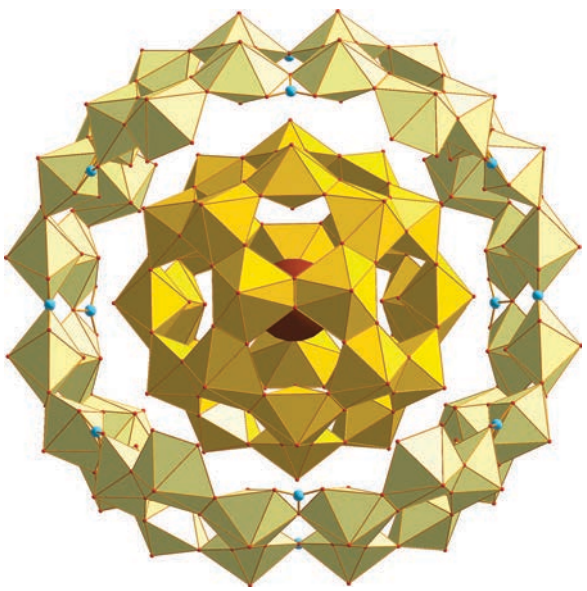

Fig. 18 Representation of the $\{U_1 \subset U_{28} \subset U_{40}R\}$ polyanion. The outside $\{U_{40}R\}$ cluster is shown in light yellow polyhedra and the middle $\{U_{28}\}$ cluster is highlighted in orange polyhedra whilst the central $\{U_1\}$ unit is presented in space filling mode. Colour code: UO_7, polyhedra; O, red spheres; N, light blue spheres. The cations and solvent molecules are omitted for clarity.

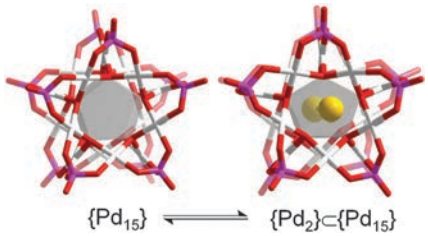

Fig. 19 Top view of the structures $[H_7Pd^{II}{}_{15}O_{10}(P^VO_4)_{10}]^{13-}$ $\{Pd_{15}\}$ and $[Pd_2{\subset}\{H_7Pd^{II}{}_{15}O_{10}(P^VO_4)_{10}\}]^{9-}$ $\{Pd_2{\subset}Pd_{15}\}$. The clusters are shown in wireframe and the central cavity is represented by a pentagon. The guest $\{Pd_2\}$ unit is shown in space filling from. Colour code: pink = P, red = O, and white = Pd.

6.3 Palladium-based POMs

The first examples of molecular palladium oxide clusters have been reported by Kortz *et al.*[77] and us. So far, a series of $\{Pd_x\}$ species of different nuclearities have been reported, namely: $\{Pd_{13}\}$, $\{Pd_{15}\}$ and a $\{Pd_{17}\}$ cluster which is a $\{Pd_{15}\}$ moiety encapsulating a $\{Pd_2\}$ dinuclear guest (Fig. 19), $\{Pd_7V_6\}$ and $\{Pd_{22}\}$.[78–82] The palladium(II) ions retain a square-planar geometry that is normally seen for Pd(II). The Pd–O distances in the range 1.95–2.09 Å are normal for Pd–O single coordination bonds and in this way the cluster could also be considered as a Pd(II) complex of AsO_4^{3-}. These clusters belong to the POM family and further developments in this chemistry *e.g.* replacement of the AsO_4^{3-} groups or even substitution of the Pd centres for other metals, could potentially lead to a large variety of new structures. Although this has gained lots of attention, due to the potential for new developments, it should be noted that *Wickleder et al.* presented a $[Pt_{12}O_8(SO_4)_{12}]^{4-}$ in 2004 which has been rarely cited.[83] More recently Kortz *et al.* successfully synthesised the first example of a POM made of gold; the polyoxoaurate $[Au^{III}{}_4As^V{}_4O_{20}]^{8-}$.[84]

7. Engineering new functionalities into POM clusters

The previously discussed novel synthetic approaches and the efforts of the synthetic chemists to move from serendipitous to designed approaches has led to a plethora of unprecedented architectures and the emergence of intriguing properties. In addition, the deep understanding of the underlying chemistry which takes place within a specific POM-based chemical system has allowed the discovery and detailed identification of the available building block libraries and better control over self-assembly processes. This process is important since the availability of the new synthetic approaches is allowing chemists to design new materials which exhibit important new properties while the deep understanding and better control of the self-assembly processes set the scene for the engineering of materials with innovative functionalities. In this section we will explore these aspects in more detail.

7.1 Homo- and heterogeneous POM – based catalysts

The diverse nature of polyoxometalates makes them attractive candidates for numerous catalytic processes. The first important physical properties are their acidity and solubility, a requisite for homogeneous catalysis, which is quite controllable for POMs as these compounds can be dissolved in aqueous as well as organic media by sensible choice of the counter cations. Moreover, the redox characteristics and the ability of the polyoxometalates to accept and release electrons in a widely variable and to some extent controllable fashion under marginal structural rearrangements, is crucial for applications in catalysis. Finally, POM-based catalysts which can be designed at the atomic/molecular level, are excellent models for the investigation of the catalytic performance and functionality of metal oxide materials by allowing the investigation of the catalytic processes at atomic/molecular level whilst they can selectively support/stabilize reaction intermediates.

Heteropolyacids (HPAs) are complex proton acids that incorporate polyoxometalate anions having metal–oxygen octahedra as the basic structural units.[5,6,85–88] The first characterized member of this family is the Keggin heteropolyanion typically represented by the formula $XM_{12}O_{40}^{y-}$ where X is the central atom (Si^{4+}, P^{5+}, *etc.*), *y* is the negative charge of the cluster and M is the metal ion (Mo^{6+} or W^{6+}). The M^{6+} ions can be substituted by many other metal ions, *e.g.* V^{5+}, Co^{2+}, Zn^{2+}, Fe^{2+} *etc.* which gives the opportunity to finely tune the relevant acidities and consequently the observed reactivity. Other polyoxometalates, *e.g.* those of the Dawson structure, $X_2M_{18}O_{62}^{y-}$; Keggin and Dawson lacunary anions, $XM_{11}O_{39}^{y-}$ and $X_2M_{17}O_{61}^{y-}$; and their transition metal complexes are also used as catalysts.[89] Among a wide variety of HPAs, the Keggin archetype is the most stable and most easily available. Indeed, Keggin based catalysts can be used in numerous catalytic processes such as oxidation catalysts for alkanes, alkenes, alcohols, aldehydes and sulphides to alcohols, ketones, epoxides, allylic alcohols, allylic ketones and sulphoxides.[90–96] Even though the molybdenum and tungsten based POMs are good acid and redox catalysts on their own, it was soon realized the potential use of transition metals as co-catalysts in order to improve their selectivity and finely tune their efficiency. For example, Mizuno *et al.* demonstrated that the cooperative effect of the mixed *addenda* $Cs_{2.5}H_{1.5}PVMo_{11}O_{40}$ Keggin compound in the presence of different transition metals. More specifically, the presence of copper cations improved the oxidation of alkanes under O_2-poor conditions considerably.[97–99] Moreover, it was demonstrated that the catalytic activity of POMs can be amplified in the presence of small inorganic anions and organic derivatives as co-catalysts or solvents.[100–103] A representative example of this cooperative effect along with the associated mechanism was investigated and reported by Neuman *et al.* where they used polyethyleneglycol (PG-200) as solvent or quinone derivatives and nitrates as co-catalysts, and improved the catalytic efficiency of the $H_5PV_2Mo_{10}O_{40}$ mixed addenda Keggin.

Research looking at POM-based catalysis has been conducted exploring the relationship between the acid or redox properties and catalytic performance as well as their unique behaviour in heterogeneous catalysis such as pseudoliquid-phase (bulk-type (I)) and the bulk-type (II) catalysis.[104–108] Since then several industrial processes have been developed which utilize heteropoly catalysts[109] such as the direct oxidation of ethylene to acetic acid catalyzed in Japanese industry where the use of palladium and HPAs as co-catalyst led to an average

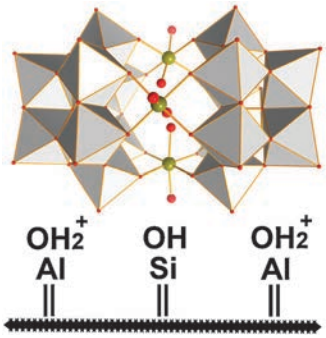

Fig. 20 Representation of the electrostatic association of $[(Fe^{III}(OH_2)_2)_3(A\text{-}\alpha\text{-}PW_9O_{34})_2]^{9-}$ with the cationic surfaces of the $(Si/AlO_2)^{n+}$ nanoparticles. The POM cluster is shown in combination polyhedral/ball-and-stick notation. Colour code: W, grey polyhedra; O, red spheres; Fe, dark yellow spheres.

production output of 100 000 tons per year. Since then lots of effort had been made to immobilize POM based catalysts on various supporting media. In 2003, Hill and co-workers reported the electrostatic immobilization of an iron derivatized polyoxometalate on cationic silica nanoparticles (Fig. 20),[110,111] which exhibits efficient catalytic activity towards the aerobic oxidation of sulphides and aldehydes under energetically efficient conditions (1 atm, room temperature).

In the work reported by Ishii *et al.* grafting an ammonium molybdovanadophosphate onto activated carbon, provided an effective and truly heterogeneous catalyst, $(NH_4)_5H_6PV_8Mo_4O_{40}/C$. The catalyst gave 46–92% yields in the oxidation of allylic and benzylic alcohols to carbonyl compounds while the control reaction showed that the unsupported POM was practically inactive.[112] In a similar fashion research groups studied the cooperative effect of immobilization of POMs on TiO_2 nanoparticles.[113] Keita *et al.* reported the light driven degradation of a highly toxic azo dye, Acid Orange 7 (AO7), by immobilization of Ni/Co-derivatized POM catalyst on TiO_2 nanoparticles.[114]

In the first efforts to tune the redox properties and acidity of the POM-based catalysts, common POM architectures were derivatized using mainly first row transitions metals (V, Ni, Co, Fe *etc.*). The development of this chemistry over the years helped research groups to gain insight into the underlying mechanism which takes place and led to the realization of a correlation between the transition elements present in the system, the isomeric forms of POM "ligands" and the activity of the synthesized catalysts. The co-operative effect by the second and third row transition metals were investigated extensively over the last decade which led to unprecedented catalytic functionalities. Palkovits and co-workers reported recently the rapid conversion of cellulose to sugar alcohols at 81% yield for C_4 to C_6 derivatives.[115] The use of the system $H_4[SiW_{12}O_{40}]/Ru$ on activated carbon proved to be effective and opened the door towards novel catalytic applications for POM-based clusters. The work reported recently by Mizuno *et al.* demonstrated another novel catalytic application for the POM clusters where the divanadium-substituted γ-phosphotungstate $TBA_4[\gamma\text{-}HPV_2W_{10}O_{40}]$ (TBA = tetra-*n*-butylammonium) in organic media acted as an effective homogeneous catalyst for the H_2O_2-based oxidative bromination of alkenes, alkynes and aromatic compounds under mild conditions.[116] The derivatization of the same material by palladium centres formed the $TBA_4[\gamma\text{-}H_2SiW_{10}O_{36}Pd_2(OAc)_2]$ cluster showed high catalytic activity for the hydration of various kinds of structurally diverse nitriles including aromatic, aliphatic, heteroaromatic and double bond-containing species.[117] More specifically, for hydration of 3-cyanopyridine, the turnover frequency was 860 h^{-1} and the turnover number reached up to 670. Finally, the reaction of $TBA_4H_4[\gamma\text{-}SiW_{10}O_{36}]$ and $Y(acac)_3$ (acac: acetylacetonato) led to the formation of an yttrium pillared silicotungstate dimer (Fig. 21) which showed significant catalytic activity for the cyanosilylation of several structurally diverse ketones and aldehydes with TMSCN which selectively proceeded to afford the corresponding cyanohydrin trimethylsilyl ethers.[118]

Work presented by Thorimbert, Lacôte and co-workers demonstrated the catalytic activity for C–C bond formation in the Diels–Alder, Mannich, and Mukaiyama-type reactions utilizing the Dawson type lacunary POM cluster. The use of lanthanide centers (La^{3+}, Eu^{3+}, Sm^{3+} and Yb^{3+}) as well as variations outside the lanthanide group (Sc^{3+}, Y^{3+}, Zr^{4+} and Hf^{4+}) has given them the opportunity to control the interplay between Lewis[119] and Brønsted acidity and consequently the observed activity of the catalysts.[120] The reported investigations led to catalysts with high chemoselectivities, consequently allowing favoured activation of imines over aldehydes.

Recently, catalytic enhancement observed with the incorporation of POMs in MOF cavities has been widely studied. For example Kholdeeva and co-workers have utilized impregnated POM/MIL-101(Cr) materials for oxidation reactions.[121,122] Even though there have been some limitations including: (a) the maximum achievable loading of POM (15 wt%) is relatively low; (b) inhomogeneity of the composite material and (c) POM leaching, POM–MOF composites have received increasing attention within the scientific community ever since the pioneering work of Zubieta.[123] Sun *et al.* described the incorporation of different POMs, $H_3XM_{12}O_{40}$ (X = Si, Ge, P and As; M = W and Mo) in the cavities of HKUST-1 resulting in the so-called NENU-*n* series.[124] The acid catalytic properties of the resulting NENU composites were explored in the hydrolysis of esters in excess water. The same group

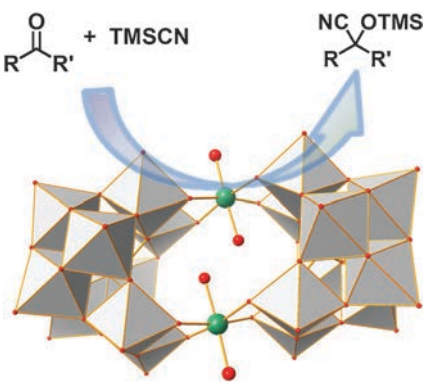

Fig. 21 Polyhedral representation of the yttrium pillared $TBA_8H_2[(SiYW_{10}O_{36})_2]$ POM dimer which was shown to be catalytically active for the cyanosilylation of ketones and aldehydes. The POM cluster is shown in a combination of polyhedral/ball-and-stick notation. Colour code: W, grey polyhedra; O, red spheres; Y, green spheres.

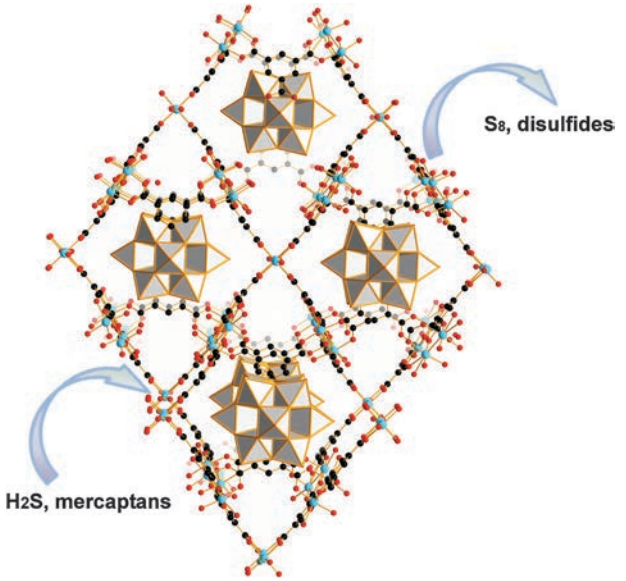

Fig. 22 Representation of the POM–MOF composite. The POM, shown in polyhedral representation, is encapsulated orientationally disordered in the pores. The MOF framework is represented in ball and stick form. Tetramethyl-ammonium (TMA) cations, which are disordered in the pores, and hydrogen atoms are omitted for clarity. Colour code: W, grey polyhedra; O, red spheres; Cu, sky blue spheres; C, black spheres.

reported that NENU-11 is an excellent candidate for eliminating nerve gas, with encapsulated $\{PW_{12}\}$ as the catalytically active centre for decomposition of type-G and type-X toxic nerve agents.[68] NENU-11 shows a rapid adsorption of dimethyl methylphosphonate (DMMP), reaching 1.92 mmol g^{-1} within 100 minutes (15.5 DMMP molecules per formula unit). The conversion of DMMP to methyl alcohol was 34% at room temperature. Furthermore, Martens *et al.* have reported the room temperature synthesis of similar POM–HKUST-1 composites and thoroughly studied their catalytic properties[125–127] for the esterification of acetic acid and 1-propanol in the absence of solvent.

More recently, Hill *et al.*[32] reported a new type of POM–MOF composites by encapsulating Cu containing phosphotungstic units $[Cu_2PW_{11}O_{39}]^{5-}$. The electrostatic interaction between POM molecules and MOF structures results in a higher reduction potential of the POM. The synergistic effect between the two structural components of the reported material extends to enhancement of stability as well as catalytic activity of the polyanions. The resulting composite material is catalytically active for the detoxification of various sulphur compounds (H_2S and mercaptans) to S_8 and disulphides using ambient air (Fig. 22). The catalyst was observed to maintain its catalytic activity for at least three cycles without significant activity loss.

7.2 POM-based molecular magnets

Polyoxometalates possess enormous diversity in both size and structure and thereby provide access to a huge library of readily available and controllable building units (BUs) that can be interconnected by electrophiles. The development of novel magnetic polyoxometalates[128] targets either the magnetic functionalization of the metal oxide fragment itself, which is mostly relevant for polyoxovanadates such as $\{V_{15}As_6\}$, $\{V_6(SO_3)_4\}$,[129,130] the interlinking of POM building blocks, as seen for $\{Mo_{72}Fe_{30}\}$,[131] $[PMo_{12}O_{40}(VO)_2]^{5-}$,[132] or the use of lacunary POM fragments as multidentate robust ligands to "trap" polynuclear paramagnetic cores (*e.g.* $\{W_{18}Cu_6\}$[133] and $\{W_{48}Cu_{20}\}$.[134] The POM ligands could be useful to "dilute" single-molecule magnets (SMMs) to remove unwanted dipolar interactions and also because of the intrinsic redox activity of the POM "ligands" allow additional routes to control magnetic-exchange pathways or introduce other functionality for device applications.[132] In addition, the POM shells are themselves surface compatible as well as being excellent ligands and SBUs allow a very high degree of reliable design and assembly that is not possible to achieve in SMMs based on first-row transition metals alone.

Even though extensive investigations have been carried out over the last two decades on the magnetic behaviour, exchange pathways and control of the spin interactions of POM-based clusters, the first Mn^{II}/Mn^{III} SMM material based on trivacant lacunary $\{B\text{-}a\text{-}X^{IV}W^{VI}_9O_{34}\}^{10-}$ polyanions has been reported only recently by us.[44] In this work, the use of two $\{B\text{-}a\text{-}XW_9O_{34}\}^{10-}$ (X = Si or Ge) polyanions to "trap" a novel mixed-valence double cubane hexanuclear $\{Mn_6\} = [Mn^{III}_4(H_2O)_2Mn^{II}_2O_4(H_2O)_2]^{8+}$ magnetic core (Fig. 23) gave rise to interesting SMM behaviour. The fitting of the experimental data with the axial zero field splitting (ZFS) plus Zeeman Hamiltonian over the whole field and temperature range gave values of $S = 5$ and $|D| = 0.67$ for the ground spin state and the anisotropic parameter respectively.

This group of compounds has been recently expanded into a promising family of materials; *e.g.* 3d-substituted POM-based compounds which exhibit SMM behaviour.[2,12,135]

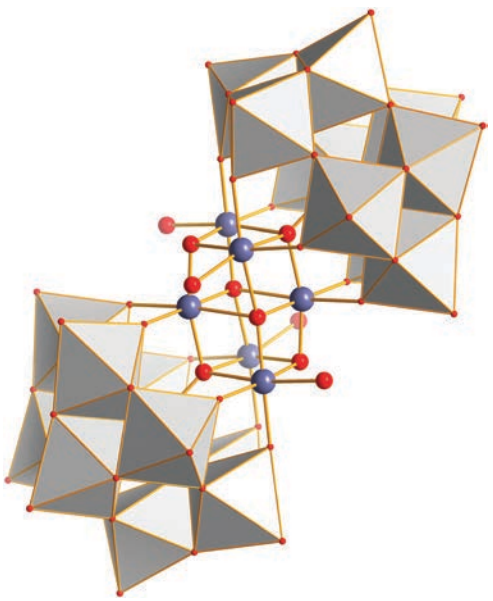

Fig. 23 Representation of the $[\{XW_9\}_2\{Mn_6\}]^{12-}$ SMM polyanion. The polyoxotungstate fragments are shown in polyhedral representation and the central $\{Mn_6O_4(OH_2)_4\}$ double-cubane core are shown as ball-and-stick. Colour code: W, grey polyhedra; O, red spheres; Mn, blue grey spheres. Counter ions and protons are omitted for clarity.

For example, Mialane *et al.* synthesized a trimeric $[(Fe_4W_9O_{34}(H_2O))_2(FeW_6O_{26})]^{19-}$ and "sandwich" type $[Fe_4(H_2O)_2(FeW_9O_{34})_2]^{10-}$ iron(III) POM clusters under hydrothermal conditions.[44] The replacement of the diamagnetic template by a transition metal (Fe^{III}) gave rise to unprecedented magnetic behaviour with ground spin states $S = 15/2$ and 5, while the relevant anisotropic parameters found to be $|D| = 0.24$ and 0.49 respectively. A couple of years later, in 2011, Kortz and co-workers reported the synthesis and characterization of the tetrameric $[\{Co_4(OH)_3PO_4\}_4(PW_9O_{34})_4]^{28-}$ nanosized cluster which encapsulates a $\{Co_{16}\}$ magnetic core.[12] The cluster synthesized under mild conditions and comprises a central $\{Co_4O_4\}$ cubane unit which is capped by four tricobalt(II)-substituted Keggin fragments $[\{Co(OH)\}_3(A\text{-}\alpha\text{-}PW_9O_{34})]^{6-}$ and four phosphate linkers, resulting in an assembly with idealized T_d symmetry and is the first example of a cobalt-core-based POM with SMM behaviour. Interpretation of the magnetic data collected below 5K gave a ground spin state value of $S = 8$ indicative for 16 Co^{II} non-interacting high spin centres.

Very recently, Mialane, Keita *et al.* expanded the family of Co-POMs which exhibit SMM behaviour. They reported the first hybrid bisphosphonate POM cluster $[\{(B\text{-}\alpha\text{-}PW_9O_{34})Co_3(OH)(H_2O)_2(O_3PC(O)(C_3H_6NH_3)PO_3)\}_2Co]^{14-}$ built of a heptanuclear Co^{II} core sandwiched by two lacunary $\{PW_9\}$ units which are connected further to two bisphosphonate ligands, each possessing a functionalizable alkyl ammonium arm.[136] Magnetic measurements showed that below 5 K the seven non-interacting Co centres ($S = \frac{1}{2}$) are coupled ferromagnetically while *M versus H* studies using an array of microSQUIDs revealed a blocking temperature of 1 K and a small value of coercive field in zero field, a phenomenon which can be attributed to fast quantum tunnelling of magnetization.

In another interesting piece of work, Kögerler *et al.* demonstrated a fruitful way to finely tune the magnetic behaviour of materials utilizing POM based building units to stabilize Mn-based clusters. More specifically, the group reported the entrapment of a Mn-cubane core using the trilacunary phospho-centred Dawson, $[\alpha\text{-}P_2W_{15}O_{56}]^{12-}$, as a robust inorganic ligand, and the characterization of the final compound, $[(\alpha\text{-}P_2W_{15}O_{56})Mn^{III}_3Mn^{IV}O_3(CH_3COO)_3]^{8-}$ (Fig. 22a).[137] Even though the double cubane motif is a common component of previously reported SMMs,[138,139] in this case they observed an unexpected zero-field splitting inversion and the subsequent loss of magnetization bistability. The careful control of the experimental variables led to a condensation product of the $\{P_2W_{15}Mn_4\}$ progenitor. In this case they managed to "switch on" the SMM behaviour by fusing together two Mn-cubane cores (Fig. 24b).[135] This is an exciting finding which demonstrates the potential of POM building units as stabilizing agents of interesting magnetic cores *via* controlled condensation during the self-assembly processes. The use of a designed approach offered in this case a great degree of control over core structures and their spin states, as demonstrated here in the construction of a heptanuclear manganese cluster with a record $S = 21/2$ ground multiplet for POM-based SMMs. The result also suggests the important consequence of the molecular symmetry and electric dipole moment on the magnetic properties of this cluster.

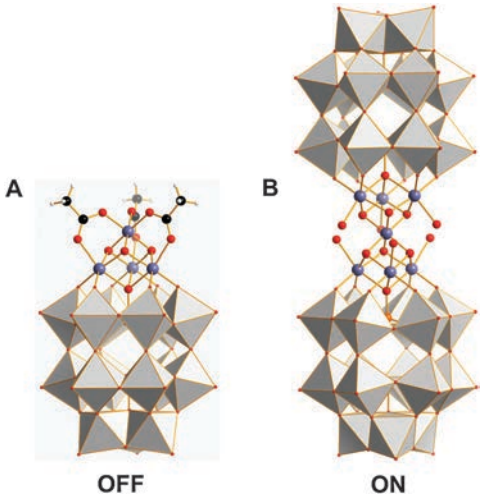

Fig. 24 Polyhedral representations of the polyoxoanion clusters with their magnetic core structures shown in ball-and-stick representation. (A) The top of the lacunary $\{P_2W_{15}\}$ fragment is decorated by the Mn-cubane core. (B) A fused di-cubane core is encapsulated between the lacunary fragments inducing SMM properties. Colour code: W, grey polyhedra; O, red spheres; Mn, blue grey spheres; C, black spheres. Counter ions are omitted for clarity.

Almost at the same period of time that the first examples of POM based SMM materials with 3d metallic cores were reported, a few very interesting studies on the interaction between POMs and lanthanides appeared in the literature. In these nanomagnets, the magnetic anisotropy responsible for the observation of slow relaxation of the magnetization arises from the zero-field splitting of the lanthanide ion's *J* ground state when it is placed in a ligand field (LF). For certain symmetries, such splitting can stabilize sublevels with a large $|Jz|$ value and consequently induces an easy axis of the magnetization. Working towards this direction, Coronado and co-workers reported the first Ln–POM based SMM in 2008 followed shortly in 2009 by an extensive investigation for a family of mononuclear Ln-based clusters.[139,140] In this piece of work, they reported the first member of the Ln–POM clusters, $[ErW_{10}O_{36}]^{9-}$ and the series of $[Ln(W_5O_{18})_2]^{9-}$ and $[Ln(\beta_2\text{-}SiW_{11}O_{39})_2]^{13-}$ (Ln^{III} = Tb, Dy, Ho, Er, Tm, and Yb) respectively. Their findings demonstrated first of all the ability of the POM "ligands" to encapsulate lanthanides by satisfying the demanding coordination sphere of the lanthanide metals due to the multiple coordination sites that they can offer. Furthermore, the group investigated the effect on the magnetic behaviour due to the introduction of an axial compression of the lanthanide centre which consequently leads to different ligand field parameters and to a change of the sign of the axial zero field splitting (ZFS) parameter of order of 2. As a consequence, the low lying excited states can be considerably different as we move across to the lanthanide series. All these initial findings such as introduction and fine adjustment of the magnetic behaviour demonstrate the potential of the polyoxometalate species for the designing of novel materials. The control of the electronic/spin state of a material is crucial for applications in quantum computing and molecular electronics.

Two years after the initial investigation of the first Ln-based single-ion magnets, Boskovic *et al.*, reported the first polynuclear

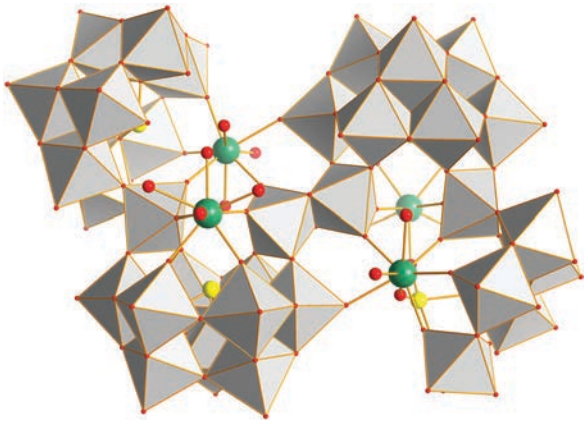

Fig. 25 Polyhedral/ball-and-stick representation of the isostructural $[Ln_4As_5W_{40}O_{144}(H_2O)_{10}(gly)_2]^{21-}$. Colour code: W, grey polyhedra; O, red spheres; As, yellow spheres; Ln, large green spheres. Counter ions are omitted for clarity.

Ln–POM based SMM compound. The use of the $[As_2W_{19}O_{67}(H_2O)]^{14-}$ as starting material in the presence of 1,4-diazabicyclooctane (DABCO) and glycine (gly) as structure directing agent led to the isolation of a family of polynuclear compounds with the general formula: $(HDABCO)_8H_5Li_8[Ln_4As_5W_{40}O_{144}(H_2O)_{10}(gly)_2]$ (Ln = Gd, Tb, Dy, Ho and Y).[141] The structure is comprised of two $\{As_2W_{19}O_{68}\}$ building blocks linked by a unit containing four rare earth ions and two additional tungsten centers, with the two glycine ligands playing a key bridging role (Fig. 25). More specifically, magnetic investigations of the Dy derivative gave an energy barrier to magnetization reversal of 3.9(1) K. Determination of the ligand field parameters indicated that the observed energy barrier arises from Ising-type magnetic anisotropy for this complex, which correlates with axial compression of the approximate local D_{4d} site symmetry at the Dy centers.

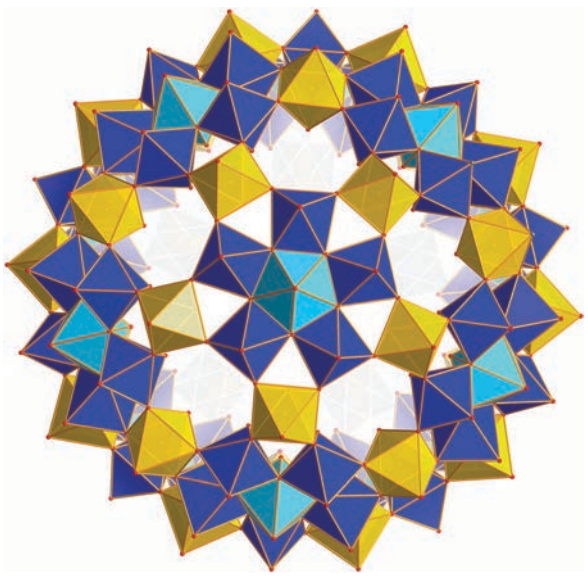

Fig. 26 Polyhedral representations of the $\{Mo_{72}Fe_{30}\}$ Keplerate polyoxoanion. The central molybdenum centre in the $\{(Mo)Mo_5\}$ fragment is highlighted as sky blue polyhedra. Colour code: Mo, blue polyhedra; O, red spheres; Fe, gold polyhedra. Counter ions are omitted for clarity.

Apart from the stabilization of interesting metallic cores, polyoxometalates revealed great potential in mediated control and tuning of the intramolecular magnetic exchange energies. In 2009, Kögerler *et al.* demonstrated how novel $\{Mo_{72}Fe_{30}\}$ Keplerate species with partially reduced $\{(Mo)Mo_5\}$ building blocks can be identified and how the 4d electron density on the still diamagnetic POM fragments strongly influences the magnetic exchange (Fig. 26).[142] The high affinity of the Keplerate-type polyoxomolybdates for transition metal linker groups, allows a complete exchange by other magnetically active linkers, such as iron(III), vanadium(IV) *etc.* or even composite materials. The whole process can be monitored by Raman spectroscopy over specific time scales during which partial oxidation of the system tunes the intramolecular magnetic interactions. Additionally, the partial reduction of the molybdate-based building blocks induces a pronounced change in the superexchange between the adjoined iron(III) centers, whilst the structure of these $\{(Mo)Mo_5\}$ electron reservoirs is fully retained.

7.3 POM-mediated processes for energy applications

Global energy consumption in the world is increasing rapidly and, although the use of fossil fuels is currently meeting our energy needs, the pressing need for a more environmentally friendly and ultimately renewable energy source is of crucial importance. It is also interesting to note that the main way biology 'fixes' sunlight *via* photosynthesis is *via* a naturally occurring polyoxometalate co-factor, the Mn-oxo unit found in the WOC. Inspired by this, there have been several important investigations aiming to develop POM-based devices and catalysts. Additionally, the unique combination of inherent properties of polyoxometalate systems, such as Lewis–Bronsted acidity, structural stability and diversity, redox properties, efficient electron and proton carries, stabilization of redox active metallic cores, *etc.* make them promising candidates for the design of POM based materials for energy related applications. For this reason, different groups over the last decades have developed methodologies for promoting the formation and trapping of novel high nuclearity architectures by employing different techniques, such as bulky organic cations to 'encapsulate' novel building blocks, thereby limiting their reorganisation to simpler structural types.[11,142–145] Also, in many cases, synthetic strategies to W- and Mo-based cluster systems are guided by the fact that structures of polyoxomolybdate clusters are frequently derived from highly stable, low nuclearity structural motifs such as the O_h-symmetric Lindqvist[85] anion $[Mo_6O_{19}]^{2-}$ and the various isomers of the Keggin structure, $[M_{12}O_{36}(XO_4)]^{n-}$ or the Dawson structure $[M_{18}O_{46}(XO_4)_2]^{n-}$ (X = S, P, As, Si *etc.*) (M = W, Mo).[85]

Taking into consideration the above new research strand, many groups focused their efforts on discovering new clusters or re-investigating the redox chemistry of previously reported compounds which could be potentially active in the water splitting/oxidation process. The first POM-based example of catalytically active species reported in 2004 by Shannon *et al.* where they investigated the redox chemistry of the di-Ru-substituted

$[WZnRu_2(OH)(H_2O)(ZnW_9O_{34})_2]^{11-}$ cluster[146] initially reported by Neuman *et al.* a few years earlier.[147] The system investigated in aqueous medium (0.1 M phosphate buffer, pH = 8) for electrochemical generation of O_2 using pulsed voltammetry. In the first set of experiments, the amount of O_2 produced was measured using a Clark sensor fabricated with a 500 μm diameter Pt disk. The di-Ru-substituted POM catalyzes the electrochemical generation of oxygen at a potential of E° = +0.760 V *vs.* SHE at pH 8 in agreement with the thermodynamics of the oxygen generation at this pH value. Interestingly, the authors compared the activity of the di-Ru sandwich cluster with the one of the mono-Ru substituted Keggin, $[XW_{11}O_{39}Ru^{III}(H_2O)]^{4-}$, cluster[148–150] which found to be inactive possibly due to spontaneous dimerization under the experimental conditions since it has been shown recently that the mono-Ru substituted Keggin species are active water catalysts. More specifically, Fukuzumi and co-workers, reported an in-depth investigation regarding the underlying mechanism of water oxidation by the single-site ruthenium heteropolytungstate clusters, $[Ru^{III}(H_2O)SiW_{11}O_{39}]^{5-}$ and $[Ru^{III}(H_2O)GeW_{11}O_{39}]^{5-}$ respectively (Fig. 27).[151] The group demonstrated by isotopic labelling, that the mono-Ru Keggin clusters in the presence of a sacrificing oxidant, $(NH_4)_2[Ce^{IV}(NO_3)_6]$, that both clusters are catalytically active over a wide range of pH values. Both complexes exhibit three one-electron redox couples based on ruthenium center. The Ru(v)–oxo complex was detected by UV-vis, EPR and Raman measurements *in situ* as an active species during the water oxidation reaction. This indicates that the Ru(v)–oxo complex is involved in the rate-determining step of the catalytic cycle of water oxidation. The overall catalytic mechanism of water oxidation was revealed on the basis of the detected catalytic intermediates. The corresponding TONs of oxygen evolution catalyzed by the Si and Ge centered clusters reached the values of 20 and 50, respectively.

Observing that the mono- and di-Ru substituted POM clusters were catalytically active in the energetically demanding process of water oxidation, the researchers focused their efforts on the incorporation of multiple ruthenium centres in the POM architecture. Indeed, in 2008, the groups of Hill *et al.*[152,153] and Bonchio *et al.*[154,155] reported independently the investigation of the Tetraruthenium(IV)–POM based homogeneous catalyst for the rapid oxidation of the water (Fig. 28). Also in this case, the POM-based lacunary building blocks allowed the incorporation and stabilization of a polynuclear ruthenium core with remarkable consequence on the cluster's catalytic activity. The independent studies from the two groups demonstrated that the tetra-Ru cluster $[\{Ru_4O_4(OH)_2(H_2O)_4\}(\gamma\text{-}SiW_{10}O_{36})_2]^{10-}$, is a robust homogeneous catalyst (500 turnovers based on the evolved oxygen) which showed a remarkable rate (maximum TOF > 450 h^{-1}). Moreover, a linear dependence of the initial rate on the concentration of the cluster is observed, with a pseudo-first-order kinetic constant of 9.92×10^{-3} s^{-1}. The following extensive physicochemical and theoretical studies reported by the two groups,[156] showed that the Ru(v)–O species are involved in the rate determining step while the nucleophilic attack of water on the high valent ruthenium centers appears to be the only reasonable mode for O–O bond formation. Additionally, intramolecular pathways, involving two molecules of catalyst, are ruled out by first-order oxygen evolution kinetics. The formation of a peroxo-ruthenium intermediate, which can finally release oxygen after a complex sequence of electron and proton transfer events, seems to be a reasonable proposition regarding the underlying mechanism which controls the whole process.

Considering that the tetra-Ru POM cluster was the most effective one, the two groups tried to modify and improve their systems and make them more energetically "independent" which will open the door for the designing devices for real applications.

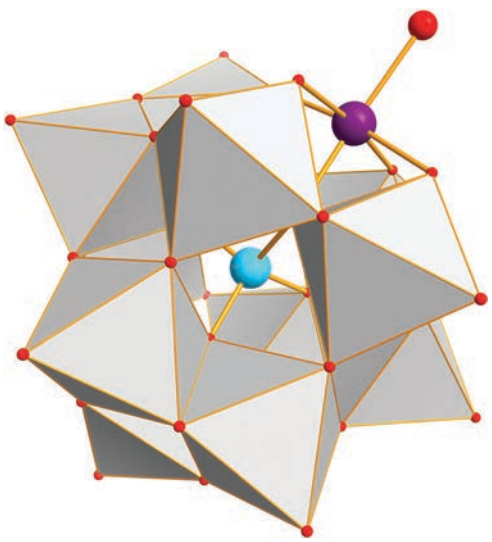

Fig. 27 Polyhedral representations of the $[Ru^{III}(H_2O)GeW_{11}O_{39}]^{5-}$ species where X = Si or Ge. Colour code: W, grey polyhedra; O, red spheres; Ru, violet polyhedra; Si/Ge, sky blue spheres. Counter ions are omitted for clarity.

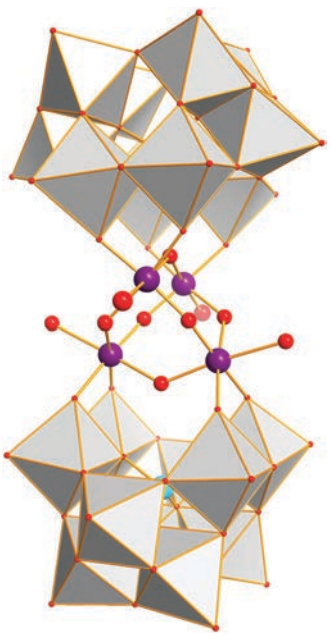

Fig. 28 Polyhedral representation of the POM-based water catalyst. The central $\{Ru_4(\mu\text{-}O)_4(\mu\text{-}OH)_2(H_2O)_4\}^{6+}$ core is shown in ball-and-stick representation. (Ru, violet spheres; O, red spheres); The polytungstate fragments are shown as grey polyhedra and Si as sky blue spheres. Counter ions and hydrogen atoms are omitted for clarity.

Indeed, they managed to use the sun light in order to give the necessary energy to the system in order to cycle between the high and low oxidations states of the Ru centres. It was shown that there is the possibility of accessing a large fraction of solar energy up to 700 nm is possible, but the maximal efficiency was estimated to be ~60% regarding the stoichiometric water oxidation by $[Ru(bpy)_3]^{3+}$ catalyzed by the cluster. This efficiency derives from a series of side reactions resulting in $[Ru(bpy)_3]^{3+}$ decomposition. Consequently, the quantum efficiencies for generating $[Ru(bpy)_3]^{3+}$ (~44%) and its reaction with the catalyst to form O_2 (~60%) are the main limiting factors in this system.[156–159]

Finally, Bonchio and co-workers,[160] reported recently their effort to design an artificial device whereby the catalytic splitting of water is finalized to give a continuous production of oxygen and hydrogen. They showed the manufacturing of an efficient and stable nanostructured, oxygen-evolving anode obtained by the assembly of the tetra-Ru oxygen-evolving polyoxometalate cluster with a conducting bed of multi-walled carbon nanotubes (MWCNTs) supported on an ITO electrode. The use of tailored and functionalized MWCNTs enables the design of water-splitting electrodes with remarkably improved efficiency, operative voltage, current density and operational stability.

In an effort to extend the investigations to materials that incorporate other metallic cores with potential interesting activity for the catalytic oxidation of water, researchers re-investigated the tetra-Co sandwich POM cluster, $[Co_4(H_2O)_2(PW_9O_{34})_2]^{10-}$, which reported for the first time by Weakley *et al.* in 1973.[161] The structure consists of a flat $\{Co_4\}$ metallic core which is trapped between two $\{PW_9O_{34}\}$ lacunary fragments of the Keggin archetype (Fig. 29).

Independent investigations by the groups of Hill[162,163] and Finke[164] demonstrated initially that the compound is active catalyst for the oxidation of water and evolution of molecular oxygen. Further detailed studies showed that the tetra-Co POM cluster can be a pre-catalyst at pH 8.0, which during the course of the electrochemical, chemical or light assisted oxidation of water, forms thin CoO_x amorphous films on the surface of the electrodes responsible for the effective catalytic activity. Nevertheless, the findings showed another exciting direction and potential use of POM based compounds which can be proved of great value in a POM assisted manufacturing approach of useful materials.

Recently, Sakai *et al.*[165] re-investigated the previously reported[166–168] Mo-based polyoxometalates containing mono- and di-cobalt(III) catalyst cores, $[CoMo_6O_{24}H_6]^{3-}$ and $[Co_2Mo_{10}O_{38}H_4]^{6-}$ (Fig. 30) and demonstrated that are active O_2-evolving catalysts in a system consisting of tris(2,20-bipyridine)ruthenium(II) ($Ru(bpy)_3^{2+}$) and sodium persulfate ($S_2O_8^{2-}$) in an aqueous media at pH 8.0. Kinetic studies demonstrated that the cobalt nuclearity is not a determining factor for the O_2 evolution rate.

The turnover numbers are estimated as 107 for Co–POM–Mo and 154 for Co2–POM–Mo based on the total amount of O_2 evolved after 30 min. In every case, the O_2 evolution reaches a plateau after 15 min of activity, which is related to the consumption of the sacrificing oxidant.

Generating hydrogen from water utilizing solar energy represents a promising and attractive way to prepare hydrogen as a clean and renewable fuel. During the past decades, significant progress has been made as hundreds of photocatalysts have been prepared and tested. Still, it is an on-going challenge to prepare efficient photocatalytic materials suitable for practical applications. The water splitting process is an electron/H^+ coupled reaction during which O_2 as well as H_2 can be evolved under appropriate conditions and POM-based materials are promising candidates for O_2 evolving applications as well as catalysts for H_2 evolution.

Recently Feng and co-workers have reported[169] the synthesis, structure, and photocatalytic properties of a new heteropolyoxoniobate, $[Nb_2O_2(H_2O)_2][SiNb_{12}O_{40}]^{10-}$. One major structural feature of the reported compound is that there is a water molecule directly coordinated to each of the two bridging Nb sites (Fig. 31). Thus, the bridging Nb metal centre is seven-coordinated with four O^{2-} anions from the Keggin cluster, two bridging O^{2-} sites shared with another Nb centre and one water molecule. The seventh coordination affects not only the local coordination geometry of the bridging Nb but also the 1-D chain configuration and packing of the chains.

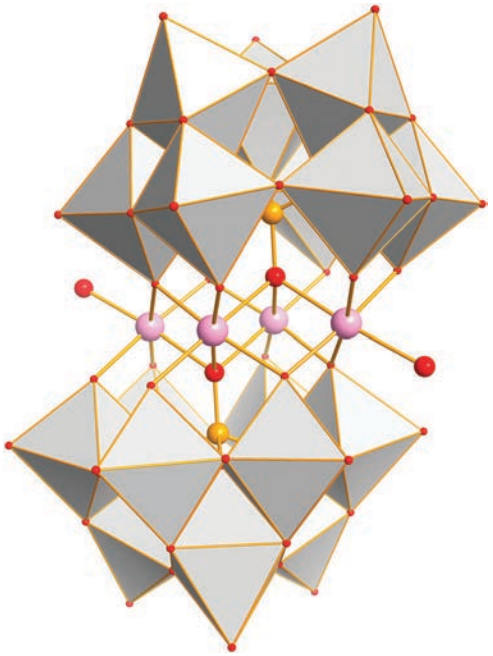

Fig. 29 Polyhedral representation of the $[Co_4(H_2O)_2(PW_9O_{34})_2]^{10-}$ Weakley sandwich cluster. The central $\{Co_4\}$ core is shown in ball-and-stick representation. (Co, pink spheres; O, red spheres); The polytungstate fragments are shown as grey polyhedra and the P atoms as light orange spheres. Counter ions and hydrogen atoms are omitted for clarity.

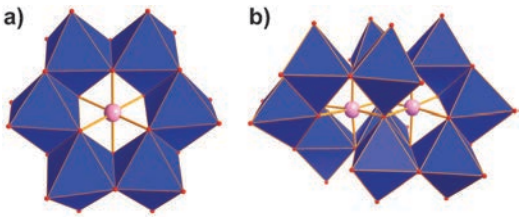

Fig. 30 Polyhedral representations of the (a) $[CoMo_6O_{24}H_6]^{3-}$ and (b) $[Co_2Mo_{10}O_{38}H_4]^{6-}$ polyoxoanions. Colour code: Mo, blue polyhedra; O, red spheres; Co, pink spheres. Counter ions are omitted for clarity.

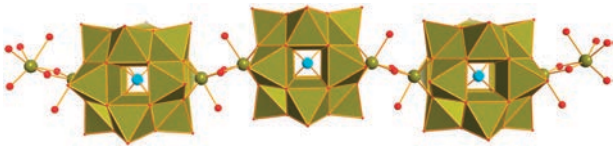

Fig. 31 Polyhedral representation of the 1-D chains of $[Nb_2O_2(H_2O)_2][SiNb_{12}O_{40}]^{10-}$. The bridging Nb appeared to be seven coordinated with one terminal water molecule occupying an axial position. Colour code: Nb, green polyhedra; O, red spheres; Si, sky blue spheres. Counter ions and protons are omitted for clarity.

The photocatalytic H_2 evolution activity of the Nb-based compound implies that the existence of an open metal site might be a new effective strategy to achieve more efficient photocatalysts. Moreover, these findings demonstrate the feasibility of using POM compounds for photocatalytic overall water-splitting reactions.

A very interesting report by Dolbecq, Draznieks, Keita *et al.*[33] demonstrates the potential of designing sophisticated architectures utilizing POMs as building units for hydrogen evolution. More specifically, they reported a series of POM-based metal organic frameworks by grafting the triangular 1,3,5-benzene tricarboxylate linkers on tetrahedral ε-Keggin polyoxometalates (POMs) capped by Zn(II) ions under hydrothermal conditions. $(TBA)_3[PMo^V_8Mo^{VI}_4O_{36}(OH)_4Zn_4][C_6H_3(COO)_3]_{4/3}\cdot 36H_2O$ exhibits a 3D open-framework architecture (Fig. 32) constructed by Keggin units connected by trim linkers, with channels occupied by tetrabutylammonium (TBA) counterions. The fabricated modified electrodes by direct adsorption of the POMOFs on glassy carbon or entrapment in carbon paste (CPE) showed exceptional activity for the electrocatalytic hydrogen evolution reaction (HER) with a yield of 95% and a TON of 1.2×10^5 was obtained after 5 h. The reported POMOF-based electrodes are more active than platinum, with a roughly 260 mV anodic shift.

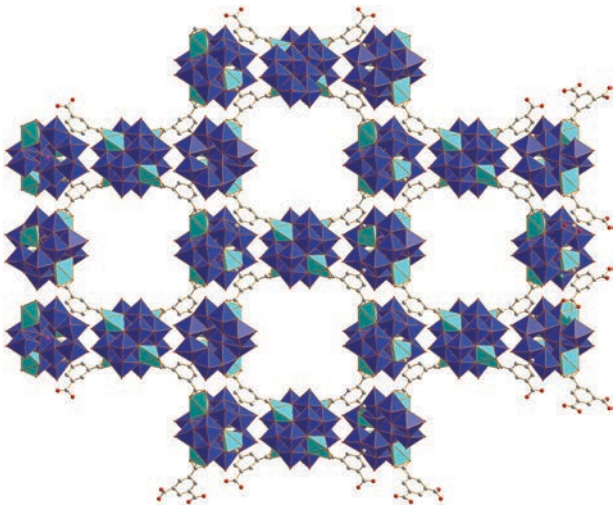

Fig. 32 Representation of the $(TBA)_3[PMo^V_8Mo^{VI}_4O_{36}(OH)_4Zn_4C_6H_3(COO)_2]$ POMOF composite. The POM is shown in polyhedral representation and the organic ligands is represented in ball and stick mode. TBA cations and hydrogen atoms are omitted for clarity. Colour code: Mo, blue polyhedra; O, red spheres; Zn, sky blue polyhedra; C, black spheres.

The fact that the compound's performance exceeds those of platinum might be associated with the structure of the POMOF and to the confinement effect. Even though the authors predicted this effect on theoretical grounds, it remains to be confirmed experimentally because the electrocatalytic properties of the POMOFs indicate that neither extensive porosity, nor the presence of conjugated ligands connecting the POMs, is required for the occurrence of the outstanding HER properties.

Finally, Floquet and co-workers reported recently[170] the use of thiometalate species as carriers of clusters which are active catalysts for the reduction of protons. More specifically, they encapsulated the complex $[Ni(dto)_2]^{2-}$ within an oxothiodecamolybdic cyclic cluster. The resulting molybdenum ring, $[Mo_{12}O_{12}S_{12}(OH)_{12}(Ni(dto)_2)]^{2-}$ possesses electrocatalytic properties for the reduction of protons and shows and alternative direction for the construction of materials which can be useful in hydrogen evolution applications. The possibility of designing functionality at the molecular level within such multicomponent systems offers promising perceptions for the fine-tuning of the electrochemical reactivity of functional materials.

7.4 Responsive POM-based archetypes for sensing applications

Organic hybrids of polyoxometalates have been increasingly attracted the attention of research groups over the past few years. Grafting organic moieties onto polyoxometallic backbones has opened up a wide structural diversity of such hybrids that possess novel properties and can allow the elaboration of unique materials or devices, as demonstrated by the characterization of surfaces patterned with covalently grafted POMs, polymers with controlled topologies or extended frameworks based on POM building units.[171–174] Interestingly the modification of POM architectures induces thermochromic and photochromic properties. This type of sensitivity to external stimuli makes them attractive for a variety of applications such as information storage media, smart windows, data display *etc.*[175]

Recently, Mialane *et al.*[176,177] demonstrated that the presence of alkylammonium groups covalently grafted on bisphosphonato ligands induces photochromic properties to ligand-coordinated polyoxomolybdate systems. Additionally their studies revealed a cooperative effect between the functionalized POM backbone, $[(Mo_3O_8)_4(O_3PC(C_3H_6NH_3)(O)PO_3)_4]^{8-}$ (Fig. 33) and the associated spyropyran (SP) counter ions. Even though has been recently reported the properties of the $(SP)_3[PM_{12}O_{40}]$ (M = W, Mo) complexes,[67] the solid state photochromic properties of this new spiropyran POM material are found to be improved considerably.

Upon UV excitation at 365 nm (3.4 eV), the colour of the POM-SP material shifts from white to reddish-brown after a few minutes. Colour change is detected, even by eye, after 1 minute of irradiation and the photoinduced colour reaches its maximum absorption coefficient after approximately one hour. A detailed investigation followed their initial effort,[178] where they reported a series of different POM-based hybrids of the general formula, $[(Mo_3O_8)_4(O_3PC(C_mH_{2m}NRR'R'')(O)PO_3)_4]^{8-}$ (m = 3; R,

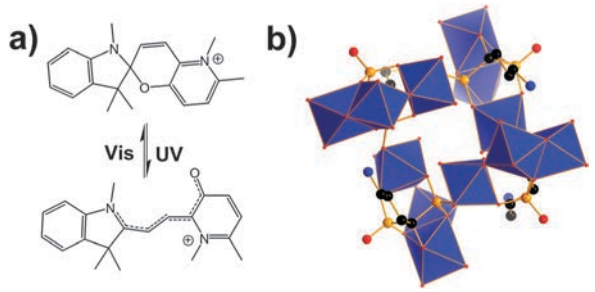

Fig. 33 (a) Representation of the closed and open form of the spiropyran countercation SP^+; (b) polyhedral and ball-and-stick representation of the $[(Mo_3O_8)_4(O_3PC(C_3H_6NH_3)(O)PO_3)_4]^{8-}$. Colour code: Mo, blue polyhedra; O, red spheres; N, blue spheres; P, light orange spheres; C, black spheres. Counter ions and protons are omitted for clarity.

R′ and R″ = H or CH_3) and $[(Mo_3O_8)_2(O)(O_3PC(C_mH_{2m}NRR'R'')(O)PO_3)_2]^{6-}$ (m = 3 or 4; R, R′ and R″ = H or CH_3) where they demonstrated the fine tuning of the photochromic properties of the materials at different wavelengths while they investigated the underlying kinetics associated with the process.

In a similar manner, Cao and co-workers[179] synthesized an organic–inorganic hybrid solid material based on cucurbituril derivative and polyoxometalate, $\{[K_2(H_2O)_2Na_2(H_2O)_2Na_2(H_2O)_6](P_2W_{18}O_{62})(Me_{10}Q_5)_2\}$ (Fig. 34), which exhibit reversible photochromic properties as well as excellent photocatalytic activities toward the degradation of methyl orange (MO) and rhodamine-B (RB) under visible light irradiation. More specifically, visible light irradiation on a fresh sample resulted in a rapid colour change within 20 min into a dark blue sample. The reverse reaction to the colourless state could be assisted by heating the material (heating at 50 °C, fast) or letting in the dark (slow, 1 day). Repeated cycling of the described process displayed good reversibility. Moreover, the materials showed excellent photocatalytic activity of methyl orange (MO) degradation under irradiation with visible light. The degradation of MO solution (10 mg L^{-1}) was completed within 180 min.

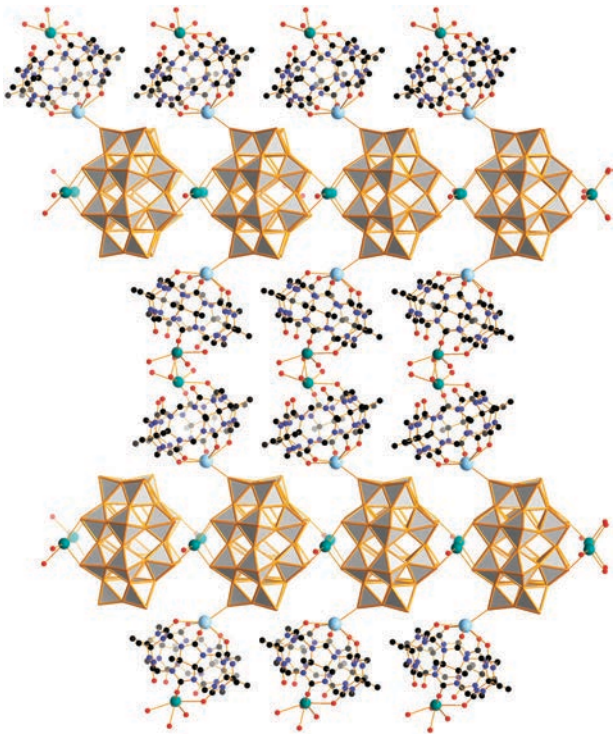

Fig. 34 Representation of the 2D structure of the composite material. The POM structure $\{P_2W_{18}O_{62}\}$ is shown in polyhedral representation while the cucurbituril moieties in ball-and-stick mode. Colour code: W, grey polyhedra; O, red spheres; N, small blue spheres; P, light orange spheres; C, small black spheres; Na, teal spheres; K, light blue spheres. Protons are omitted for clarity.

Utilizing a different type of stimulus, Hasenknopf, Lacôte, Rieger *et al.* the first organo-POM with thermoresponsive properties reported recently.[180] They synthesized a POM–polymer which was prepared by grafting poly(*N*,*N*-diethylacrylamine) PDEAAm-NH_2 onto the activated Dawson acyl-POM, a_2-$[P_2W_{17}O_{61}SnCH_2CH_2C(=O)]^{6-}$. Aqueous solutions of the $(NH_4)_7$[POM–PDEAAm] exhibited a lower solution critical temperature (LCST) of 38 °C. Consequently, the solubility/aggregation of the hybrid was reversibly controlled by changing the temperature. Above 38 °C, the solution became cloudy and cleared again upon cooling. Upon heating the solution the POM–polymer composite forms aggregations which their size depends on the LCST. The lower the temperature is the smaller sized aggregations can be obtained. The findings demonstrate the significance of POM–hybrid composites in the field of materials chemistry and sizing of functional nanoparticles.

A few years ago, we[39] reported an interesting case of a POM-based material which showed responsiveness as a function of the temperature. In this case the emergence of the property did not arise from the cooperative effect between the POM backbone and an organic moiety. In this case the Dawson type cluster, β-$[Mo^{VI}_{18}O_{54}(SO_3)_2]^{4-}$ encapsulates two sulphite anions, with a short S···S contact resulting from the incorporation and relative orientation of the two sulphite anions within the $\{Mo_{18}\}$ cage. However, preliminary studies showed thermochromic behaviour at 77 and 500 K (Fig. 35), which represented the first report of such behaviour for discrete polyoxometalate clusters. These initial investigations also showed that the colour changes are gradual and are completely reversible between pale yellow (77 K) and deep red (500 K).

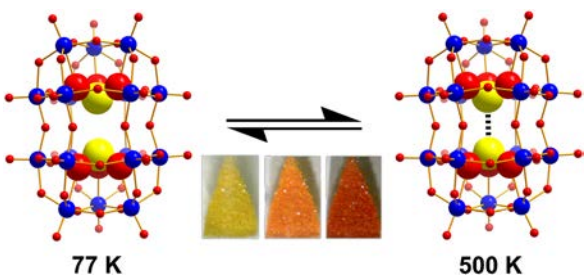

Fig. 35 Ball-and-stick representation of the $[Mo_{18}O_{54}(SO_3)_2]^{4-}$ POM cage. As the temperature increases to 500 K a gradual colour change is observed. Colour code: Mo, blue; O, red; S, yellow. Counter ions are omitted for clarity.

7.5 Ionic POMs – batteries and super-capacitors

Energy conversion devices such as fuel cells and renewable energy devices such as photovoltaic or dye-sensitized solar cells demand the presence of an efficient way to store the produced energy. For this purpose have been studied numerous conducting polymers and metal oxide polymers as well as composite materials of all the above in order to take advantage on the potential co-operative effect.[181] Owing to their diverse nature in terms of architecture and properties, polyoxometalates are the missing link between the chemistry of bulk, extended metal oxide solids and the chemistry of monomeric molecules, and this provides further opportunities to isolate electroactive as well as multifunctional materials. Hybrids based on polyoxometalates provide a case study of the importance to target specific applications for specific materials such as electrode cathodes,[182,183] batteries and super-capacitors.[184]

The Mo-Keggin structure is a common starting point for investigating the properties of POM-based composite materials, especially for the development of novel electrode materials for batteries. Recently Yoshikawa, Awaga *et al.* reported a detailed investigation on the valence and structural changes of the POM during the charging–discharging process.[183] Specifically, they carried out in operando Mo K-edge X-ray absorption fine structure measurements on the rechargeable molecular cluster batteries (MCBs) of POMs in which the Keggin-type POM is utilized as a cathode active material with a lithium metal anode. They showed that the material exhibited a large capacity of *ca.* 270 (A h) kg^{-1} in a voltage range of 1.5–4.0 V. X-ray absorption near-edge investigation demonstrated that all 12 Mo^{6+} metal centres are reduced to Mo^{4+} in the discharging process which means that the cluster can store 24 electrons (Fig. 36) and carry a negative charge of 27- and explains the observed large capacity. This extended electron sponge behaviour is an important newly revealed characteristic of POMs and indicates that they are promising cathode active materials for high-performance rechargeable batteries.

Taking into account the ability of POM-based materials to store and release electrons under specific conditions, make them excellent candidates for the design of composite hybrid materials which exhibit interesting cooperative effects for energy storage and behave as super-capacitors. Also in this case, the Keggin structure is a popular choice due to its excellent stability, acidity and redox properties. Recently, Fransaer *et al.*,[184] synthesized composite materials synthesized by reacting 1-butyl-3-methylimidazolium tetrafluoroborate (BMIM) ionic liquid and $H_4SiW_{12}O_{40}{\cdot}nH_2O$ or $H_3PMo_{12}O_{40}{\cdot}nH_2O$ which were used to form homogeneous films using AC electrophoretic deposition. The materials exhibited specific capacitance of 172 F g^{-1} for $(BMIM)_4SiW_{12}O_{40}$ and 89 F g^{-1} for $(BMIM)_3PMo_{12}O_{40}$, respectively.

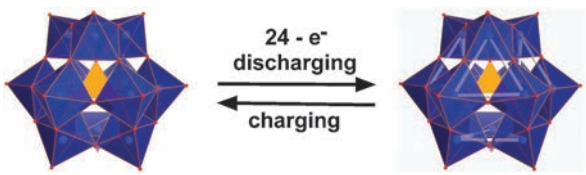

Fig. 36 Polyhedral representation of the molecular structure of $[PMo_{12}]^{3-}$ (LEFT) and model molecular structure of $[PMo_{12}]^{27-}$ during the charging–discharging process. The formed metal–metal bonds during the discharging process are highlighted white. Colour code: Mo, blue polyhedra; O, red spheres; P, light orange polyhedra. Counter ions are omitted for clarity.

A lot of work has been done in the preparation of composite materials using conducting polymers and POMs. The integration of polyoxometalates in conducting polymers led to the development of a new class of electroactive hybrids which resulted in a new concept material for application in electrochemical supercapacitors.[185,186] Gómez-Romero and co-workers prepared the molecular hybrids, PAni/$H_4SiW_{12}O_{40}$, PAni/$H_3PW_{12}O_{40}$ and PAni/$H_3PMo_{12}O_{40}$ (PAni: Polyaniline), which exhibited the ability to store and release charge in solid state capacitors with a specific capacitance of 120 F g^{-1} and cyclability over 1000 cycles.[185]

Another interesting example of POM-based composite materials reported by the same group, is the preparation of a material based on multiwalled carbon nanotubes (CNT) and phosphomolybdate polyanion (Cs-PMo_{12}) using polyvinyl acetate (PVA) as binder. In this case they achieved even higher capacitance values of up to 285 F g^{-1} a considerable increase on the energy density compared with pure CNT electrodes and stability of 500 cycles.[187]

From a different point of view, the composite materials made of polyoxometalates and molecular cations can create ionic crystals with specific structures.[188] Controlling the shape, size, and charge of the POMs, it is possible to predetermine their arrangement and create molecular-sized spaces in the crystal lattice. The cooperative effect of ionic crystals with cations can give rise to accessible space within the otherwise densely packed crystal lattice by reducing the Coulomb interactions, may induce surface and guest sorption properties different form inorganic zeolites and organic coordination polymers whilst may enable the heterogeneous catalysis in the crystal lattice. In the case of coordination polymers, there is difficulty in the creation of coordinatively unsaturated metal sites for the catalytic reaction and the catalysis of coordination polymers remains largely unexplored.

Following the above designed approach, Gómez-García, Giménez-Saiz *et al.* reported the synthesis of two new radical salts formed by the organic donors bis(ethylenedithio)-tetrathiafulvalene (ET) and bis(ethylenediseleno)tetrathiafulvalene (BETS) and the Keggin polyoxometalate (POM) $[SMo_{12}O_{40}]^{n-}$. At ambient pressure $ET_8[SMo_{12}O_{40}]$ is a classical semiconductor with a room temperature conductivity of 1 S cm^{-1} and an activation energy of about 130 meV while $BETS_8[SMo_{12}O_{40}]$ (Fig. 37) exhibits an activated behaviour although it does not follow a classical semiconducting regime.[189] In the case where W-based Keggin POMs were used instead as anionic components, $ET_8[SiMo_{12}O_{40}]$, $ET_8[CoMo_{12}O_{40}]$ and $ET_8[BMo_{12}O_{40}]$, they observed semiconducting behaviour with room temperature conductivities of 0.15, 0.07, and 0.03 S cm^{-1} and activation energies of 94, 119, and 159 meV respectively (Fig. 37).[190]

Recently we, along with Nakamura and co-workers,[191] reported the crystal structure and physical properties (magnetic and ionic conductivity) of a new gigantic $\{Mo_{176}\}$-wheel containing Co^{II} and Fe^{III} ions as the external charge

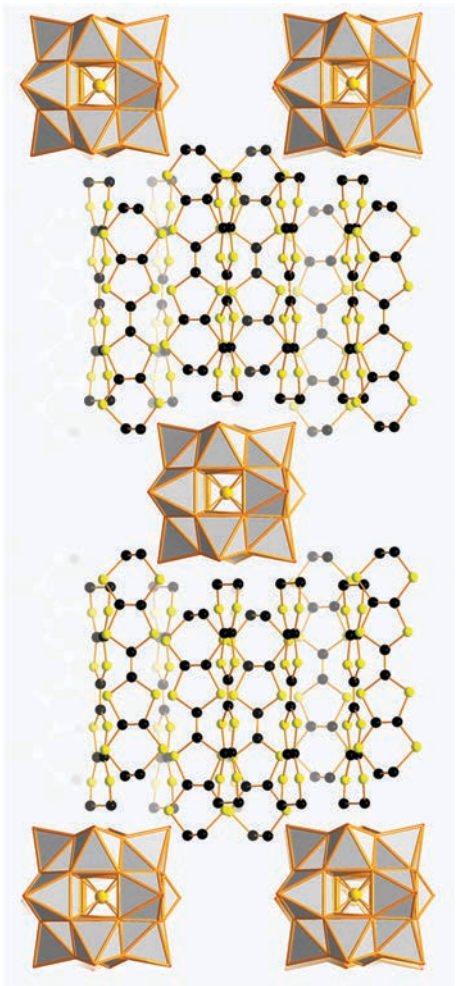

Fig. 37 Polyhedral/ball-and-stick representation of the molecular structure of $ET_8[BW_{12}O_{40}]$. Colour code: W, grey polyhedra; O, red spheres; S, yellow spheres; C: black spheres; B, light orange spheres. Counter ions and protons are omitted for clarity.

balancing counter cations in addition to Na cations. In this case the stacking of the wheels filled with disordered Na^+, Fe^{III}, Co^{II} and H_2O species facilitated the observed conductivity instead of the π–π stacking ability of an aromatic molecule. More specifically, the ionic conductivity of a single crystal at 300 K was 3×10^{-7} S cm^{-1} with activation energy of 0.43 eV. Also, Mizuno and co-workers, reported recently the preparation of two ionic compounds with specific porosity by controlling carefully the electrostatic interactions of the anionic (POM) and cationic part of the composite material in the space.[22] X-ray diffraction studies of the single crystal produced by the single-step reaction of heterometallic M_2Zn_2-substituted POMs (M = Co^{II} or Ni^{II}) and an assembly of these heterometallic substituted POMs with tetrabutylammonium (TBA) cations into porous ionic crystals with the following general formula $[\{M(OH_2)_2(\mu_3\text{-}OH)\}_2\ \{Zn(OH_2)\}_2\{\gamma\text{-}HSiW_{10}O_{36}\}_2]^{8-}$. In this case the strong electrostatic interactions formed well-defined $58 \times 58 \times 58$ Å^3 and $38 \times 38 \times 38$ Å^3 spherical voids and demonstrated the high mobility of the guest molecules which can be exchanged without jeopardising the porous structural integrity of the materials. This interesting finding demonstrates the potential of this approach for the design of catalytic materials with specific reactivity. The practical application of this approach is the report of the ionic porous material reported by the same group,[192] of the formula $[Cr_3O(OOCCH_2X)_6(H_2O)_3]_4[\alpha\text{-}SiW_{12}O_{40}]$, (X = Cl or Br), where they showed a propylene/propane and ethylene/ethane sorption ratios at 298 K and 100 kPa of 6.1 and 3.6, respectively and these values are much larger than those of conventional sorbents.

8. Transformation of POM structures at interfaces

The structural diversity and flexibility of polyoxometalates means that they have a special position in inorganic chemistry. Their intrinsic anionic nature, ability to bridge multiple length scales, be involved with multiple redox processes that can be modulated, as well as their multiple functionalities mean that they can show new and unexpected properties. For instance we recently observed that it is possible to re-fabricate crystals of polyoxometalates *via* a type of material morphogenesis giving novel physical tubular structures *via* an osmotic process.[193] Similar to the classical crystal garden, whereby a crystal of a transition metal salt is placed in a concentrated solution of sodium silicate, the immersion of a crystal of a polyoxometalate in a solution of an organo-cation gives rise to this process. This is interesting since this emergent effect occurs in a system that is dissipative *i.e.* a dynamic ion exchange process resulting in the (re-)precipitation of the cluster.[194] In fact, we showed that microtubes can be spontaneously grown from crystals of POM-based materials when immersed in solutions containing dihydroimidazophenanthridinium (DIP) cations (Fig. 38) with variable growth rates (1–100 μm S^{-1}) and with high aspect ratios (> 10 000).

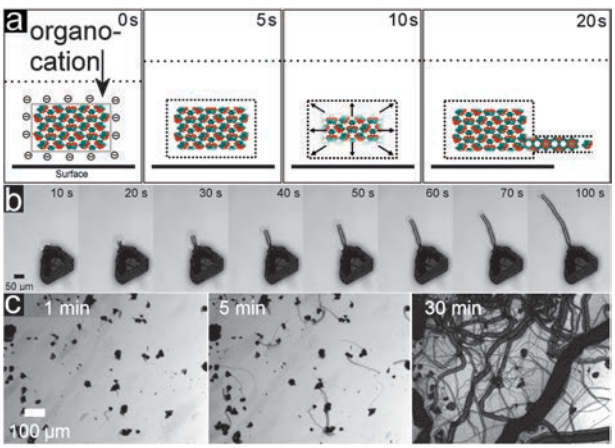

Fig. 38 Spontaneous tube formation from POM crystals. (a) Schematic representation of the initial processes giving rise to the emergence of tubes; addition of a solution of organic cations to a POM crystal results in the formation of a semi-permeable membrane around the crystal. The crystal then dissolves within the membrane and creates an osmotic pressure. The membrane ruptures and a tube is formed as dissolved fragments of the POM come into contact with the solution of the cation. (b) Time-lapse images of a single tube emerging from a crystal. (c) Images showing a large number of crystals giving rise to many tubes in a bulk system.

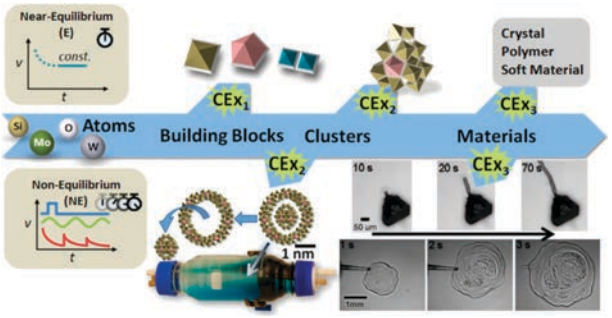

Fig. 39 A depiction of the cation exchange process (CExn) for the assembly of building blocks, clusters and materials to be developed in this research. Further, trapping the objects under NE conditions allows the development of a range of highly sophisticated molecules and materials. These are shown by three key examples recently discovered by us: (i) assembly of a nanowheel, complete with transient template under flow; (ii) growth of tubes from POM crystals; (iii) assembly of POM-based membrane sacks.

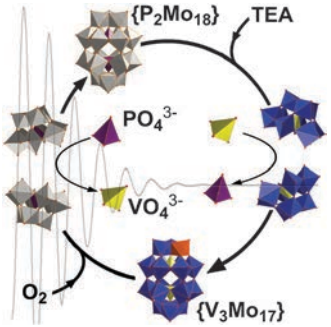

Fig. 40 The POM-oscillator showing the redox driven guest change reaction. Colour scheme: PO_4^{3-} templated cluster, grey; VO_4^{3-} templated cluster, blue; PO_4^{3-}, purple; VO_4^{3-}, template yellow; reduced V, orange.

The transformation of the crystals into tubes occurs when a solution of a bulky cation on a sparsely soluble crystal starts to dissolve and a membrane forms, and this can even be observed using ion-change measurements as well as optical microscopy using an ion-sensitive-field-effect-transistor sensor array.[195] The membrane formation is mediated by the aggregation of the large organo-cations with the large POM anions and this then sets up the osmotic process leading to the tubes, formed by membrane rupture. As water influx maintains a constant flow of material through the opening, tubes are formed and it is even possible to steer the tubes.[196] Also, the development of tubes from pellets of the POM and using inert modifiers is also possible.[197] Additionally, we can predict the solubility limits of tube growth and have used this to produce a set of rules explaining if a given POM/cation combinations will undergo morphogenesis to produce tubes. Furthermore, if we inject a solution of the POM, rather than dropping a crystal into the solution of the cation, it is possible to produce POM-based 'inorganic cells'.[198] These inorganic chemical cells or iCHELLS are important since they are able to separate assembly processes, reactions, select the inclusion or exclusion of ions on the basis of size and contrast the ion-exchange process occurring at a solid–liquid interface compared to that occurring at a liquid–liquid interface, see Fig. 39.

9. Conclusions and outlook

One of the key aspects of the new developments at the frontiers of metal oxide cluster science is based on that the finding that cluster structures are built on a hierarchy of template and templating subunits, yet this not yet explored in detail. Also, it is only just emerging that reaction networks based upon polyoxometalates can be increasingly treated as complex chemical systems containing interdependent networks of self-assembling, self-templating building blocks. Indeed, complex interacting 'systems' defined using polyoxometalate building blocks may be used as the archetypal models to explore inorganic chemical networks.

The area of polyoxometalates is now entering into a new phase whereby it is possible to design and control both the structure and function of the systems. However their dynamic nature with a seemingly endless structural diversity means that the assembly of functional nano-molecules and adaptive materials under non-equilibrium conditions will be developed. This approach will be used to access new building block libraries which will lead to the formation of novel nano-material structures and functions not accessible from near equilibrium processing techniques and will be focused on producing new materials, assemblies and devices. Such processes may be driven using redox reactions, ion exchange, metal unit substitution, to drive, direct and trap the self-assembly of molecular metal oxide based building blocks, clusters, and materials in solution. By using such non-equilibrium based processing, it will be possible aim to engineer materials with unprecedented structures functionality and adaptive potential than possible with conventional, static, near equilibrium self-assembly techniques. For example, in very recent work we have shown that it is possible to engineer cluster–guest compounds whereby an cluster-based oscillator is engineered whereby the oscillation in the internal cluster template can be driven by the presence of a reducing amine in solution, and the oxidation of the solution let open to the atmosphere, see Fig. 40.[199] The fact that such dynamic behaviour can be set up and observed in solution is exciting, and the coupling of such processes between the solution and solid-state has fantastic promise for the future design and discovery of polyoxometalate-based reaction systems and networks with emergent properties. We are confident that the structural explosion in the area of polyoxometalates will now lead to an explosion in functionality taking advantage of the transferable building blocks, ability to engineer non-equilibrium systems with unprecedented properties and emergent functionalities.

Acknowledgements

The authors would like to thank the University of Glasgow, WestCHEM, the EPSRC, Leverhulme Trust, the Royal Society/Wolfson Foundation, the Royal Society of Edinburgh and Marie Curie actions for financial support as well as members of the Cronin laboratory, past and present. We would like to thank Mr Thomas Boyd for comments on the manuscript.

References

1 *Polyoxometalate Chemistry for Nanocomposite Design*, ed. M. T. Pope and T. Yamase, Kluwer, Dordrecht, 2002.
2 J.-D. Compain, P. Mialane, A. Dolbecq, I. M. Mbomekalle, J. Marrot, F. Sécheresse, E. Rivière, G. Rogez and W. Wernsdorfer, *Angew. Chem., Int. Ed.*, 2009, **48**, 3077.
3 N. Mizuno, K. Yamaguchi and K. Kamata, *Coord. Chem. Rev.*, 2005, **249**, 1944.
4 J. T. Rhule, C. L. Hill and D. A. Judd, *Chem. Rev.*, 1998, **98**, 327.
5 M. T. Pope and A. Müller, *Angew. Chem., Int. Ed. Engl.*, 1991, **30**, 34.
6 *Special issue on polyoxometalates*, ed. C.L. Hill, *Chem. Rev.*, 1998, **98**, 1.
7 D.-L. Long, E. Burkholder and L. Cronin, *Chem. Soc. Rev.*, 2007, **36**, 105.
8 D.-L. Long, R. Tsunashima and L. Cronin, *Angew. Chem., Int. Ed.*, 2010, **49**, 1736.
9 E. Ahmed and M. Ruck, *Angew. Chem., Int. Ed.*, 2012, **51**, 308.
10 M. D. Symes, P. J. Kitson, J. Yan, C. J. Richmond, G. J. T. Cooper, R. W. Bowman, T. Vilbrandt and L. Cronin, *Nat. Chem.*, 2012, **4**, 349.
11 D.-L. Long, P. Kögerler, L. J. Farrugia and L. Cronin, *Angew. Chem., Int. Ed.*, 2003, **42**, 4180.
12 M. Ibrahim, Y. Lan, B. S. Bassil, Y. Xiang, A. Suchopar, A. K. Powell and U. Kortz, *Angew. Chem., Int. Ed.*, 2011, **50**, 4708.
13 C. P. Pradeep, D.-L. Long, P. Kögerler and L. Cronin, *Chem. Commun.*, 2007, 4254.
14 B. S. Bassil, M. Ibrahim, R. Al-Oweini, M. Asano, Z. Wang, J. van Tol, N. S. Dalal, K.-Y. Choi, R. Ngo Biboum, B. Keita, L. Nadjo and U. Kortz, *Angew. Chem., Int. Ed.*, 2011, **50**, 5961.
15 S. G. Mitchell, P. I. Molina, S. Khanra, H. N. Miras, A. Prescimone, G. J. T. Cooper, R. S. Winter, E. K. Brechin, D.-L. Long, R. J. Cogdell and L. Cronin, *Angew. Chem., Int. Ed.*, 2011, **50**, 9154.
16 G. W. Brudvig, *Coord. Chem. Rev.*, 2008, **252**, 231.
17 N. Leclerc-Laronze, J. Marrot, R. Thouvenot and E. Cadot, *Angew. Chem., Int. Ed.*, 2009, **48**, 4986.
18 F. Hussain, F. Conrad and G. R. Patzke, *Angew. Chem., Int. Ed.*, 2009, **48**, 9088.
19 C. Ritchie, E. G. Moore, M. Speldrich, P. Kögerler and C. Boskovic, *Angew. Chem., Int. Ed.*, 2010, **49**, 7702.
20 X. K. Fang and P. Kögerler, *Angew. Chem., Int. Ed.*, 2008, **47**, 8123.
21 X. Fang, P. Kögerler, Y. Furukawa, M. Speldrich and M. Luban, *Angew. Chem., Int. Ed.*, 2011, **50**, 5212.
22 K. Suzuki, Y. Kikukawa, S. Uchida, H. Tokoro, K. Imoto, S.-I. Ohkoshi and N. Mizuno, *Angew. Chem., Int. Ed.*, 2012, **51**, 1597.
23 N. Mizuno, S. Uchida, K. Kamata, R. Ishimoto, S. Nojima, K. Yonehara and Y. Sumida, *Angew. Chem., Int. Ed.*, 2010, **49**, 9972.
24 K. Uehara and N. Mizuno, *J. Am. Chem. Soc.*, 2011, **133**, 1622.
25 C. Besson, J.-H. Mirebeau, S. Renaudineau, S. Roland, S. Blanchard, H. Vezin, C. Courillon and A. Proust, *Inorg. Chem.*, 2011, **50**, 2501.
26 C. Besson, D. G. Musaev, V. Lahootun, R. Cao, L.-M. Chamoreau, R. Villanneau, F. Villain, R. Thouvenot, Y. V. Geletii, C. L. Hill and A. Proust, *Chem.–Eur. J.*, 2009, **15**, 10233.
27 G. Izzet, E. Ishow, J. Delaire, C. Afonso, J. C. Tabet and A. Proust, *Inorg. Chem.*, 2009, **48**, 11865.
28 V. Lahootun, C. Besson, R. Villanneau, F. Villain, L.-M. Chamoreau, K. Boubekeur, S. Blanchard, R. Thouvenot and A. Proust, *J. Am. Chem. Soc.*, 2007, **129**, 7127.
29 C. Ritchie, C. Streb, J. Thiel, S. G. Mitchell, H. N. Miras, D.-L. Long, T. Boyd, R. D. Peacock, T. McGlone and L. Cronin, *Angew. Chem., Int. Ed.*, 2008, **47**, 6881.
30 C. Lydon, C. Busche, H. N. Miras, A. Delf, D.-L. Long, L. Yellowlees and L. Cronin, *Angew. Chem., Int. Ed.*, 2012, **51**, 2115.
31 C. P. Pradeep, D.-L. Long, C. Streb and L. Cronin, *J. Am. Chem. Soc.*, 2008, **130**, 14946.
32 J. Song, Z. Luo, D. K. Britt, H. Furukawa, O. M. Yaghi, K. I. Hardcastle and C. L. Hill, *J. Am. Chem. Soc.*, 2011, **133**, 16839.
33 B. Nohra, H. El Moll, L. M. Rodriguez Albelo, P. Mialane, J. Marrot, C. Mellot-Draznieks, M. O'Keeffe, R. N. Biboum, J. Lemaire, B. Keita, L. Nadjo and A. Dolbecq, *J. Am. Chem. Soc.*, 2011, **133**, 13363.
34 F. H. Aidoudi, D. W. Aldous, R. J. Goff, A. M. Z. Slawin, J. P. Attfield, R. E. Morris and P. Lightfoot, *Nat. Chem.*, 2011, **3**, 801.
35 S. Lin, W. Liu, Y. Li, Q. Wu, E. Wang and Z. Zhang, *Dalton Trans.*, 2010, **39**, 1740.
36 C. P. Pradeep, D.-L. Long and L. Cronin, *Dalton Trans.*, 2010, **39**, 9443.
37 D.-L. Long, H. Abbas, P. Kögerler and L. Cronin, *J. Am. Chem. Soc.*, 2004, **126**, 13880.
38 J. Yan, D.-L. Long, H. N. Miras and L. Cronin, *Inorg. Chem.*, 2010, **49**, 1819.
39 D.-L. Long, P. Kögerler and L. Cronin, *Angew. Chem., Int. Ed.*, 2004, **43**, 1817.
40 H. N. Miras, D. J. Stone, E. J. L. McInnes, R. G. Raptis, P. Baran, G. I. Chilas, M. P. Sigalas, T. A. Kabanos and L. Cronin, *Chem. Commun.*, 2008, 4703.
41 H. Abbas, A. L. Pickering, D.-L. Long, P. Kögerler and L. Cronin, *Chem.–Eur. J.*, 2005, **11**, 1071.
42 D.-L. Long, P. Kögerler, A. D. C. Parenty, J. Fielden and L. Cronin, *Angew. Chem., Int. Ed.*, 2006, **45**, 4798.
43 C. Ritchie, T. Boyd, D.-L. Long, E. Ditzel and L. Cronin, *Dalton Trans.*, 2009, 1587.
44 C. Ritchie, A. Ferguson, H. Nojiri, H. N. Miras, Y. F. Song, D.-L. Long, E. Burkholder, M. Murrie, P. Kögerler, E. K. Brechin and L. Cronin, *Angew. Chem., Int. Ed.*, 2008, **47**, 5609.
45 X. M. Zhang, H. S. Wu, F. Q. Zhang, A. Prikhod'ko, S. Kuwata and P. Comba, *Chem. Commun.*, 2004, 2046.
46 E. R. Cooper, C. D. Andrews, P. S. Wheatley, P. B. Webb, P. Wormald and R. E. Morris, *Nature*, 2004, **430**, 1012.
47 A. S. Pakhomova and S. V. Krivovichev, *Inorg. Chem. Commun.*, 2010, **13**, 1463.
48 H. N. Miras, G. J. T. Cooper, D.-L. Long, H. Bögge, A. Müller, C. Streb and L. Cronin, *Science*, 2010, **327**, 72.
49 H. N. Miras, C. J. Richmond, D.-L. Long and L. Cronin, *J. Am. Chem. Soc.*, 2012, **134**, 3816.
50 M. Ibrahim, S. S. Mal, B. S. Bassil, A. Banerjee and U. Kortz, *Inorg. Chem.*, 2011, **50**, 956.
51 J. Yan, D.-L. Long and L. Cronin, *Angew. Chem., Int. Ed.*, 2010, **49**, 4117.
52 J. Yan, J. Gao, D.-L. Long, H. N. Miras and L. Cronin, *J. Am. Chem. Soc.*, 2010, **132**, 11410.
53 J. Gao, J. Yan, S. G. Mitchell, H. N. Miras, A. G. Boulay, D.-L. Long and L. Cronin, *Chem. Sci.*, 2011, **2**, 1502.
54 M. N. Corella-Ochoa, H. N. Miras, A. Kidd, D.-L. Long and L. Cronin, *Chem. Commun.*, 2011, **47**, 8799.
55 J. Gao, J. Yan, S. Beeg, D.-L. Long and L. Cronin, *Angew. Chem., Int. Ed.*, 2012, **51**, 3373.
56 J. Thiel, D. Yang, M. H. Rosnes, X. Liu, C. Yvon, S. E. Kelly, Y.-F. Song, D.-L. Long and L. Cronin, *Angew. Chem., Int. Ed.*, 2011, **50**, 8871.
57 D.-L. Long, Y. F. Song, E. F. Wilson, P. Kögerler, S. X. Guo, A. M. Bond, J. S. J. Hargreaves and L. Cronin, *Angew. Chem., Int. Ed.*, 2008, **47**, 4384.
58 J. Yan, D.-L. Long, E. F. Wilson and L. Cronin, *Angew. Chem., Int. Ed.*, 2009, **48**, 4376.
59 L. Vila-Nadal, S. G. Mitchell, D.-L. Long, A. Rodriguez-Fortea, X. Lopez, J. M. Poblet and L. Cronin, *Dalton Trans.*, 2012, **41**, 2264.
60 J. Thiel, C. Ritchie, C. Streb, D.-L. Long and L. Cronin, *J. Am. Chem. Soc.*, 2009, **131**, 4180.
61 J. Thiel, C. Ritchie, H. N. Miras, C. Streb, S. G. Mitchell, T. Boyd, M. N. C. Ochoa, M. H. Rosnes, J. McIvet, D.-L. Long and L. Cronin, *Angew. Chem., Int. Ed.*, 2010, **49**, 6984.
62 S. G. Mitchell, C. Streb, H. N. Miras, T. Boyd, D.-L. Long and L. Cronin, *Nat. Chem.*, 2010, **2**, 308.
63 L. Zhang and W. Schmitt, *J. Am. Chem. Soc.*, 2011, **133**, 11240.
64 J. M. Breen and W. Schmitt, *Angew. Chem., Int. Ed.*, 2008, **47**, 6904.
65 S.-T. Zheng, J. Zhang, X.-X. Li, W.-H. Fang and G.-Y. Yang, *J. Am. Chem. Soc.*, 2010, **132**, 15102.

66 (*a*) P. Mialane, A. Dolbecq, L. Lisnard, A. Mallard, J. Marrot and F. Secheresse, *Angew. Chem., Int. Ed.*, 2002, **41**, 2398; (*b*) A. Dolbecq, E. Dumas, C. R. Mayer and P. Mialane, *Chem. Rev.*, 2010, **110**, 6009.
67 L. Marleny Rodriguez-Albelo, A. Rabdel Ruiz-Salvador, A. Sampieri, D. W. Lewis, A. Gomez, B. Nohra, P. Mialane, J. Marrot, F. Secheresse, C. Mellot-Draznieks, R. N. Biboum, B. Keita, L. Nadjo and A. Dolbecq, *J. Am. Chem. Soc.*, 2009, **131**, 16078.
68 F.-J. Ma, S.-X. Liu, C.-Y. Sun, D.-D. Liang, G.-J. Ren, F. Wei, Y.-G. Chen and Z.-M. Su, *J. Am. Chem. Soc.*, 2011, **133**, 4178.
69 C. Zou, Z. Zhang, X. Xu, Q. Gong, J. Li and C.-D. Wu, *J. Am. Chem. Soc.*, 2012, **134**, 87.
70 R. P. Bontchev and M. Nyman, *Angew. Chem., Int. Ed.*, 2006, **45**, 6670.
71 R. Tsunashima, D.-L. Long, H. N. Miras, D. Gabb, C. P. Pradeep and L. Cronin, *Angew. Chem., Int. Ed.*, 2010, **49**, 113.
72 C. A. Ohlin, E. M. Villa, J. C. Fettinger and W. H. Casey, *Angew. Chem., Int. Ed.*, 2008, **47**, 5634.
73 M. Nyman, *Dalton Trans.*, 2011, **40**, 8049.
74 Y. Hou, M. Nyman and M. A. Rodriguez, *Angew. Chem., Int. Ed.*, 2011, **50**, 12514.
75 G. E. Sigmon, D. K. Unruh, J. Ling, B. Weaver, M. Ward, L. Pressprich, A. Simonetti and P. C. Burns, *Angew. Chem., Int. Ed.*, 2009, **48**, 2737.
76 (*a*) G. E. Sigmon and P. C. Burns, *J. Am. Chem. Soc.*, 2011, **133**, 9137; (*b*) J. Qiu, J. Ling, A. Sui, J. E. S. Szymanowski, A. Simonetti and P. C. Burns, *J. Am. Chem. Soc.*, 2012, **134**, 1810; (*c*) J. Ling, C. M. Wallace, J. E. S. Szymanowski and P. C. Burns, *Angew. Chem., Int. Ed.*, 2010, **49**, 7271.
77 E. V. Chubarova, M. H. Dickman, B. Keita, L. Nadjo, F. Miserque, M. Mifsud, I. Arends and U. Kortz, *Angew. Chem., Int. Ed.*, 2008, **47**, 9542.
78 F. Xu, R. A. Scullion, J. Yan, H. N. Miras, C. Busche, A. Scandurra, B. Pignataro, D.-L. Long and L. Cronin, *J. Am. Chem. Soc.*, 2011, **133**, 4684.
79 N. V. Izarova, R. N. Biboum, B. Keita, M. Mifsud, I. W. C. E. Arends, G. B. Jameson and U. Kortz, *Dalton Trans.*, 2009, 9385.
80 M. Delferro, C. Graiff, L. Elviri and G. Predieri, *Dalton Trans.*, 2010, **39**, 4479.
81 N. V. Izarova, N. Vankova, A. Banerjee, G. B. Jameson, T. Heine, F. Schinle, O. Hampe and U. Kortz, *Angew. Chem., Int. Ed.*, 2010, **49**, 7807.
82 M. Barsukova-Stuckart, N. V. Izarova, G. B. Jameson, V. Ramachandran, Z. Wang, J. van Tol, N. S. Dalal, R. Ngo Biboum, B. Keita, L. Nadjo and U. Kortz, *Angew. Chem., Int. Ed.*, 2011, **50**, 2639.
83 M. Pley and M. S. Wickleder, *Angew. Chem., Int. Ed.*, 2004, **43**, 4168.
84 N. V. Izarova, N. Vankova, T. Heine, R. N. Biboum, B. Keita, L. Nadjo and U. Kortz, *Angew. Chem., Int. Ed.*, 2010, **49**, 1886.
85 M. T. Pope, *Heteropoly and Isopoly Oxometalates*, Springer-Verlag, 1983.
86 J. D. Dunitz, P. Hemmerich, R. H. Holm, J. A. Ibers, C. K. Jorgensen, J. B. Neilands, D. Reinen and R. J. P. Williams, *Structure and Bonding vol. 18 large molecules*, 1974.
87 J. F. Keggin, *Proc. R. Soc. London, Ser. A*, 1934, **A144**, 75.
88 A. Müller and M. T. Pope, *Polyoxometalates – from platonic solids to anti-retroviral activity*, Kluwer Academic Publishers, Dordrecht, London, 1994.
89 J. E. Lyons, P. E. Ellis Jr., H. K. Myers Jr., G. Suld and W. A. Langdale, *U.S. Patent 4803187*, Feb. 7, 1989.
90 B. S. Dzhumakaeva and W. A. Golodov, *J. Mol. Catal.*, 1986, **35**, 303.
91 R. Neumann and M. Levin, *J. Org. Chem.*, 1991, **56**, 5707.
92 R. Neumann and M. Lissel, *J. Org. Chem.*, 1989, **54**, 4607.
93 (*a*) M. K. Harrup and C. L. Hill, *Inorg. Chem.*, 1994, **33**, 5448; (*b*) M. K. Harrup and C. L. Hill, *J. Mol. Catal. A: Chem.*, 1996, **106**, 57.
94 R. Neumann and M. Levin, in *Dioxygen Activation and Homogeneous Catalytic Oxidation*, ed. L. I. Simandi, Elsevier, Amsterdam, 1991, p. 121.
95 R. Neumann and C. Abugnim, *J. Chem. Soc., Chem. Commun.*, 1989, 1324.
96 R. Neumann and C. Abugnim, *J. Am. Chem. Soc.*, 1990, **112**, 6025.
97 N. Mizuno, W. C. Han and T. Kudo, *J. Catal.*, 1998, **178**, 391.
98 N. Mizuno, D. J. Suh, W. Han and T. Kudo, *J. Mol. Catal. A: Chem.*, 1996, **114**, 309.
99 N. Mizuno, W. Han and T. Kudo, *Chem. Lett.*, 1996, 1121.
100 A. Haimov and R. Neumann, *Chem. Commun.*, 2002, 876.
101 R. Neumann, A. M. Khenkin and I. Vigdergauz, *Chem.–Eur. J.*, 2000, **6**, 875.
102 *Polyoxometalate Chemistry: From Topology via self-assembly to applications*, ed. M. T. Pope and A. Müller, Kluwer Academic Publishers, Dordrecht, 2001.
103 A. M. Khenkin and R. Neumann, *J. Am. Chem. Soc.*, 2004, **126**, 6356.
104 M. Misono and N. Nojiri, *Appl. Catal.*, 1990, **64**, 1.
105 A. Corma, *Chem. Rev.*, 1995, **95**, 559.
106 Y. Izumi, *Catal. Today*, 1997, **33**, 371.
107 I. V. Kozhevnikov, *Catal. Rev.*, 1995, **37**, 311.
108 T. Okuhara, N. Mizuno and M. Misono, *Adv. Catal.*, 1996, **41**, 113.
109 N. Nojiri and M. Misono, *Appl. Catal., A*, 1993, **93**, 103.
110 N. M. Okun, T. M. Anderson and C. L. Hill, *J. Am. Chem. Soc.*, 2003, **125**, 3194.
111 N. M. Okun, M. D. Ritorto, T. M. Anderson, R. P. Apkarian and C. L. Hill, *Chem. Mater.*, 2004, **16**, 2551.
112 S. Fujibayashi, K. Nakayama, M. Hamamoto, S. Sakaguchi, Y. Nishiyama and Y. Ishii, *J. Mol. Catal. A: Chem.*, 1996, **110**, 105.
113 M. Yoon, J. A. Chang, Y. Kim, J. R. Choi, K. Kim and S. J. Lee, *J. Phys. Chem. B*, 2001, **105**, 2539.
114 R. N. Biboum, C. P. N. Njiki, G. Zhang, U. Kortz, P. Mialane, A. Dolbecq, I. M. Mbomekalle, L. Nadjo and B. Keita, *J. Mater. Chem.*, 2011, **21**, 645.
115 R. Palkovits, K. Tajvidi, A. M. Ruppert and J. Procelewska, *Chem. Commun.*, 2011, **47**, 576.
116 K. Yonehara, K. Kamata, K. Yamaguchi and N. Mizuno, *Chem. Commun.*, 2011, **47**, 1692.
117 T. Hirano, K. Uehara, K. Kamata and N. Mizuno, *J. Am. Chem. Soc.*, 2012, **134**, 6425.
118 Y. Kikukawa, K. Suzuki, M. Sugawa, T. Hirano, K. Kamata, K. Yamaguchi and N. Mizuno, *Angew. Chem., Int. Ed.*, 2012, **51**, 2434.
119 H. El Moll, B. Nohra, P. Mialane, J. Marrot, N. Dupre, B. Riflade, M. Malacria, S. Thorimbert, B. Hasenknopf, E. Lacote, P. A. Aparicio, X. Lopez, J. M. Poblet and A. Dolbecq, *Chem.–Eur. J.*, 2011, **17**, 14129.
120 N. Dupre, P. Remy, K. Micoine, C. Boglio, S. Thorimbert, E. Lacote, B. Hasenknopf and M. Malacria, *Chem.–Eur. J.*, 2010, **16**, 7256.
121 G. Ferey, C. Mellot-Draznieks, C. Serre, F. Millange, J. Dutour, S. Surble and I. Margiolaki, *Science*, 2005, **309**, 2040.
122 (*a*) N. V. Maksimchuk, M. N. Timofeeva, M. S. Melgunov, A. N. Shmakov, Y. A. Chesalov, D. N. Dybtsev, V. P. Fedin and O. A. Kholdeeva, *J. Catal.*, 2008, **257**, 315; (*b*) N. V. Maksimchuk, K. A. Kovalenko, S. S. Arzumanov, Y. A. Chesalov, M. S. Melgunov, A. G. Stepanov, V. P. Fedin and O. A. Kholdeeva, *Inorg. Chem.*, 2010, **49**, 2920.
123 (*a*) D. Hagrman, C. Zubieta, D. J. Rose, J. Zubieta and R. C. Haushalter, *Angew. Chem., Int. Ed. Engl.*, 1997, **36**, 873; (*b*) P. J. Hagrman, D. Hagrman and J. Zubieta, *Angew. Chem., Int. Ed.*, 1999, **38**, 2639.
124 C.-Y. Sun, S.-X. Liu, D.-D. Liang, K.-Z. Shao, Y.-H. Ren and Z.-M. Su, *J. Am. Chem. Soc.*, 2009, **131**, 1883.
125 L. H. Wee, S. R. Bajpe, N. Janssens, I. Hermans, K. Houthoofd, C. E. A. Kirschhock and J. A. Martens, *Chem. Commun.*, 2010, **46**, 8186.
126 L. H. Wee, N. Janssens, S. R. Bajpe, C. E. A. Kirschhock and J. A. Martens, *Catal. Today*, 2011, **171**, 275.
127 M. Mustafa, J. Ollier, J. Simpson, M. A. Riley, E. S. Paul, X. Wang, A. Aguilar, M. P. Carpenter, I. G. Darby, D. J. Hartley, R. V. F. Janssens, F. G. Kondev, T. Lauritsen, P. J. Nolan, M. Petri, J. M. Rees, J. P. Revill, S. V. Rigby, C. Teal, J. Thomson, C. Unsworth, S. Zhu, B. G. Carlsson, H. L. Ma, T. Mufti and I. Ragnarsson, *Phys. Rev. C: Nucl. Phys.*, 2011, **84**, 054320.

128 A. Muller, F. Peters, M. T. Pope and D. Gatteschi, *Chem. Rev.*, 1998, **98**, 239.
129 D. Gatteschi, L. Pardi, A. L. Barra, A. Müller and J. Doring, *Nature*, 1991, **354**, 463.
130 M. J. Manos, H. N. Miras, V. Tangoulis, J. D. Woollins, A. M. Z. Slawin and T. A. Kabanos, *Angew. Chem., Int. Ed.*, 2003, **42**, 425.
131 A. Muller, M. Luban, C. Schroder, R. Modler, P. Kögerler, M. Axenovich, J. Schnack, P. C. Canfield, S. Bud'ko and N. Harrison, *ChemPhysChem*, 2001, **2**, 517.
132 J. Lehmann, A. Gaita-Arino, E. Coronado and D. Loss, *Nat. Nanotechnol.*, 2007, **2**, 312.
133 T. Yamase, K. Fukaya, H. Nojiri and Y. Ohshima, *Inorg. Chem.*, 2006, **45**, 7698.
134 S. S. Mal and U. Kortz, *Angew. Chem., Int. Ed.*, 2005, **44**, 3777.
135 X. Fang, P. Kögerler, M. Speldrich, H. Schilder and M. Luban, *Chem. Commun.*, 2012, **48**, 1218.
136 H. El Moll, A. Dolbecq, J. Marrot, G. Rousseau, M. Haouas, F. Taulelle, G. Rogez, W. Wernsdorfer, B. Keita and P. Mialane, *Chem.–Eur. J.*, 2012, **18**, 3845.
137 X. K. Fang, M. Speldrich, H. Schilder, R. Cao, K. P. O'Halloran, C. L. Hill and P. Kögerler, *Chem. Commun.*, 2010, **46**, 2760.
138 S. M. J. Aubin, M. W. Wemple, D. M. Adams, H. L. Tsai, G. Christou and D. N. Hendrickson, *J. Am. Chem. Soc.*, 1996, **118**, 7746.
139 M. A. AlDamen, J. M. Clemente-Juan, E. Coronado, C. Marti-Gastaldo and A. Gaita-Arino, *J. Am. Chem. Soc.*, 2008, **130**, 8874.
140 M. A. AlDamen, S. Cardona-Serra, J. M. Clemente-Juan, E. Coronado, A. Gaita-Arino, C. Marti-Gastaldo, F. Luis and O. Montero, *Inorg. Chem.*, 2009, **48**, 3467.
141 C. Ritchie, M. Speldrich, R. W. Gable, L. Sorace, P. Kögerler and C. Boskovic, *Inorg. Chem.*, 2011, **50**, 7004.
142 B. Botar, A. Ellern, R. Hermann and P. Kögerler, *Angew. Chem., Int. Ed.*, 2009, **48**, 9080.
143 D.-L. Long, P. Kögerler, L. J. Farrugia and L. Cronin, *Dalton Trans.*, 2005, 1372.
144 D.-L. Long, D. Orr, G. Seeber, P. Kögerler, L. J. Farrugia and L. Cronin, *J. Cluster Sci.*, 2003, **14**, 313.
145 (*a*) M. T. Pope, in *Comprehensive Coordination Chemistry*, ed. G. Wilkinson, R. D. Gillard and J. A. McCleverty, Pergamon Press, 1987, vol. 3, p. 1023; (*b*) in *Polyoxometalate Molecular Science*, ed. J. J. Borrás-Almenar, E. Coronado, A. Müller and M. T. Pope, Kluwer Academic Publishers, Dordrecht, The Netherlands, 2003.
146 A. R. Howells, A. Sankarraj and C. Shannon, *J. Am. Chem. Soc.*, 2004, **126**, 12258.
147 R. Neumann and A. M. Khenkin, *Inorg. Chem.*, 1995, **34**, 5753.
148 M. Sadakane and M. Higashijima, *Dalton Trans.*, 2003, 659.
149 M. Sadakane, D. Tsukuma, M. H. Dickman, B. Bassil, U. Kortz, M. Higashijima and W. Ueda, *Dalton Trans.*, 2006, 4271.
150 M. Sadakane, D. Tsukuma, M. H. Dickman, B. S. Bassil, U. Kortz, M. Capron and W. Ueda, *Dalton Trans.*, 2007, 2833.
151 M. Murakami, D. C. Hong, T. Suenobu, S. Yamaguchi, T. Ogura and S. Fukuzumi, *J. Am. Chem. Soc.*, 2011, **133**, 11605.
152 Y. V. Geletii, B. Botar, P. Koegerler, D. A. Hillesheim, D. G. Musaev and C. L. Hill, *Angew. Chem., Int. Ed.*, 2008, **47**, 3896.
153 Y. V. Geletii, C. Besson, Y. Hou, Q. S. Yin, D. G. Musaev, D. Quinonero, R. Cao, K. I. Hardcastle, A. Proust, P. Kögerler and C. L. Hill, *J. Am. Chem. Soc.*, 2009, **131**, 17360.
154 A. Sartorel, M. Carraro, G. Scorrano, R. De Zorzi, S. Geremia, N. D. McDaniel, S. Bernhard and M. Bonchio, *J. Am. Chem. Soc.*, 2008, **130**, 5006.
155 A. Sartorel, P. Miró, E. Salvadori, S. Romain, M. Carraro, G. Scorrano, M. Di Valentin, A. Llobet, C. Bo and M. Bonchio, *J. Am. Chem. Soc.*, 2009, **131**, 16051.
156 Y. V. Geletii, Z. Q. Huang, Y. Hou, D. G. Musaev, T. Q. Lian and C. L. Hill, *J. Am. Chem. Soc.*, 2009, **131**, 7522.
157 C. Besson, Z. Q. Huang, Y. V. Geletii, S. Lense, K. I. Hardcastle, D. G. Musaev, T. Q. Lian, A. Proust and C. L. Hill, *Chem. Commun.*, 2010, **46**, 2784.
158 M. Orlandi, R. Argazzi, A. Sartorel, M. Carraro, G. Scorrano, M. Bonchio and F. Scandola, *Chem. Commun.*, 2010, **46**, 3152.
159 F. Puntoriero, G. La Ganga, A. Sartorel, M. Carraro, G. Scorrano, M. Bonchio and S. Campagna, *Chem. Commun.*, 2010, **46**, 4725.
160 F. M. Toma, A. Sartorel, M. Iurlo, M. Carraro, P. Parisse, C. Maccato, S. Rapino, B. R. Gonzalez, H. Amenitsch, T. Da Ros, L. Casalis, A. Goldoni, M. Marcaccio, G. Scorrano, G. Scoles, F. Paolucci, M. Prato and M. Bonchio, *Nat. Chem.*, 2010, **2**, 826.
161 T. J. R. Weakley, H. T. Evans, J. S. Showell, G. F. Tourné and C. M. Tourné, *J. Chem. Soc., Chem. Commun.*, 1973, 139.
162 Q. S. Yin, J. M. Tan, C. Besson, Y. V. Geletii, D. G. Musaev, A. E. Kuznetsov, Z. Luo, K. I. Hardcastle and C. L. Hill, *Science*, 2010, **328**, 342.
163 Z. Q. Huang, Z. Luo, Y. V. Geletii, J. W. Vickers, Q. S. Yin, D. Wu, Y. Hou, Y. Ding, J. Song, D. G. Musaev, C. L. Hill and T. Q. Lian, *J. Am. Chem. Soc.*, 2011, **133**, 2068.
164 J. J. Stracke and R. G. Finke, *J. Am. Chem. Soc.*, 2011, **133**, 14872.
165 S. Tanaka, M. Annaka and K. Sakai, *Chem. Commun.*, 2012, **48**, 1653.
166 A. Perloff, *Inorg. Chem.*, 1970, **9**, 2228.
167 H. T. Evans and J. S. Showell, *J. Am. Chem. Soc.*, 1969, **91**, 6881.
168 K. Nomiya, M. Wada, H. Murasaki and M. Miwa, *Polyhedron*, 1987, **6**, 1343.
169 Z. Y. Zhang, Q. P. Lin, D. Kurunthu, T. Wu, F. Zuo, S. T. Zheng, C. J. Bardeen, X. H. Bu and P. Y. Feng, *J. Am. Chem. Soc.*, 2011, **133**, 6934.
170 A. Hijazi, J. C. Kemmegne-Mbouguen, S. Floquet, J. Marrot, C. R. Mayer, V. Artero and E. Cadot, *Inorg. Chem.*, 2011, **50**, 9031.
171 Y. F. Song, N. McMillan, D.-L. Long, S. Kane, J. Malm, M. O. Riehle, C. P. Pradeep, N. Gadegaard and L. Cronin, *J. Am. Chem. Soc.*, 2009, **131**, 1340.
172 M. Lu, W. A. Nolte, T. He, D. A. Corley and J. M. Tour, *Chem. Mater.*, 2009, **21**, 442.
173 J. Kang, B. B. Xu, Z. H. Peng, X. D. Zhu, Y. G. Wei and D. R. Powell, *Angew. Chem., Int. Ed.*, 2005, **44**, 6902.
174 J. W. Han and C. L. Hill, *J. Am. Chem. Soc.*, 2007, **129**, 15094.
175 (*a*) M. Irie, *Chem. Rev.*, 2000, **100**, 1683; (*b*) H. Dürr and H. Bouas-Laurent, in *Photochromism: Molecules and Systems*, Elsevier, Amsterdam, 2003.
176 J. D. Compain, P. Deniard, R. Dessapt, A. Dolbecq, O. Oms, F. Secheresse, J. Marrot and P. Mialane, *Chem. Commun.*, 2010, **46**, 7733.
177 P. Mialane, G. J. Zhang, I. M. Mbomekalle, P. Yu, J. D. Compain, A. Dolbecq, J. Marrot, F. Secheresse, B. Keita and L. Nadjo, *Chem.–Eur. J.*, 2010, **16**, 5572.
178 H. El Moll, A. Dolbecq, I. M. Mbomekalle, J. Marrot, P. Deniard, R. Dessapt and P. Mialane, *Inorg. Chem.*, 2012, **51**, 2291.
179 J. Lu, J. X. Lin, X. L. Zhao and R. Cao, *Chem. Commun.*, 2012, **48**, 669.
180 in *Structure and Bonding*, ed. N. D. Chasteen, M. J. Clarke, J. B. Goodenough, J. A. Ibers, C. K. Jørgensen, D. M. P. Mingos, J. B. Neilands, G. A. Palmer, D. Reinen, P. J. Sadler, R. Weiss and R. J. P. Williams, Springer-Verlag, New York, 1983, vol. 53, p. 105.
181 (*a*) P. Gomez-Romero and C. Sanchez, in *Functional hybrid materials*, Wiley-VCH, Weinheim, 2004; (*b*) P. Gomez-Romero, *Adv. Mater.*, 2001, **13**(3), 163.
182 (*a*) M. Lira-Cantú and P. Gómez-Romero, *Chem. Mater.*, 1998, **10**, 698; (*b*) P. Gómez-Romero and M. Lira-Cantú, *Adv. Mater.*, 1997, **9**(2), 144.
183 H. Wang, S. Hamanaka, Y. Nishimoto, S. Irle, T. Yokoyama, H. Yoshikawa and K. Awaga, *J. Am. Chem. Soc.*, 2012, **134**, 4918.
184 M. Ammam and J. Fransaer, *J. Electrochem. Soc.*, 2011, **158**, A14.
185 A. K. Cuentas-Gallegos, M. Lira-Cantú, N. Casañ-Pastor and P. Gómez-Romero, *Adv. Funct. Mater.*, 2005, **15**, 1125.
186 P. Gómez-Romero, M. Chojak, A. K. Cuentas-Gallegos, J. A. Asensio, P. J. Kulesza, N. Casañ-Pastor and M. Lira-Cantú, *Electrochem. Commun.*, 2003, **5**, 149.
187 A. K. Cuentas-Gallegos, R. Martínez-Rosales, M. Baibarac, P. Gómez-Romero and M. E. Rincón, *Electrochem. Commun.*, 2007, **9**, 2088.
188 S. Uchida and N. Mizuno, *Coord. Chem. Rev.*, 2007, **251**, 2537.
189 E. Coronado, S. Curreli, C. Giménez-Saiz, C. J. Gómez-García, A. Alberola and E. Canade, *Inorg. Chem.*, 2009, **48**, 11314.

190 C. J. Gómez-García, C. Giménez-Saiz, S. Triki, E. Coronado, P. Le Magueres, L. Ouahab, L. Ducasse, C. Sourisseau and P. Delhaes, *Inorg. Chem.*, 1995, **34**, 4139.
191 H. Imai, T. Akutagawa, F. Kudo, M. Ito, K. Toyoda, S.-I. Noro, L. Cronin and T. Nakamura, *J. Am. Chem. Soc.*, 2009, **131**, 13578.
192 S. Uchida, R. Eguchi, S. Nakamura, Y. Ogasawara, N. Kurosawa and N. Mizuno, *Chem. Mater.*, 2012, **24**, 325.
193 C. Ritchie, G. J. T. Cooper, Y.-F. Song, C. Streb, H. Yin, A. D. C. Parenty, D. A. MacLaren and L. Cronin, *Nat. Chem.*, 2009, **1**, 47.
194 G. J. T. Cooper, A. G. Boulay, P. J. Kitson, C. Ritchie, C. J. Richmond, J. Thiel, D. Gabb, R. Eadie, D.-L. Long and L. Cronin, *J. Am. Chem. Soc.*, 2011, **133**, 5947.
195 B. Nemeth, M. D. Symes, A. G. Boulay, C. Busche, G. J. T. Cooper, D. R. S. Cumming and L. Cronin, *Adv. Mater.*, 2012, **24**, 1238.
196 G. J. T. Cooper and L. Cronin, *J. Am. Chem. Soc.*, 2009, **131**, 8368.
197 A. G. Boulay, G. J. T. Cooper and L. Cronin, *Chem. Commun.*, 2012, **48**, 5088.
198 G. J. T. Cooper, P. J. Kitson, R. S. Winter, M. Zagnoni, D.-L. Long and L. Cronin, *Angew. Chem., Int. Ed.*, 2011, **50**, 10373.
199 H. N. Miras, M. Sorus, J. Hawkett, D. O. Sells, E. J. L. McInnes and L. Cronin, *J. Am. Chem. Soc.*, 2012, **134**, 6980.

